Supporting Information

A Bifunctional NAD$^+$ for Profiling Poly-ADP-Ribosylation-Dependent Interacting Proteins

Albert T. Lam[a,†], Xiao-Nan Zhang[a,†], Valentine V. Courouble[b], Timothy S. Strutzenberg[b], Hua Pei[c], Bangyan L. Stiles[a], Stan G. Louie[c], Patrick R. Griffin[b], and Yong Zhang[a,d,e,f*]

[a] Department of Pharmacology and Pharmaceutical Sciences, School of Pharmacy, University of Southern California, Los Angeles, CA 90089

[b] Department of Molecular Medicine, The Scripps Research Institute, Jupiter, FL 33458

[c] Titus Family Department of Clinical Pharmacy, School of Pharmacy, University of Southern California, Los Angeles, CA 90089

[d] Department of Chemistry, Dornsife College of Letters, Arts and Sciences, University of Southern California, Los Angeles, CA 90089

[e] Norris Comprehensive Cancer Center, University of Southern California, Los Angeles, CA 90089

[f] Research Center for Liver Diseases, University of Southern California, Los Angeles, CA 90089

[†] These authors contributed equally to this work.

* Email: yongz@usc.edu

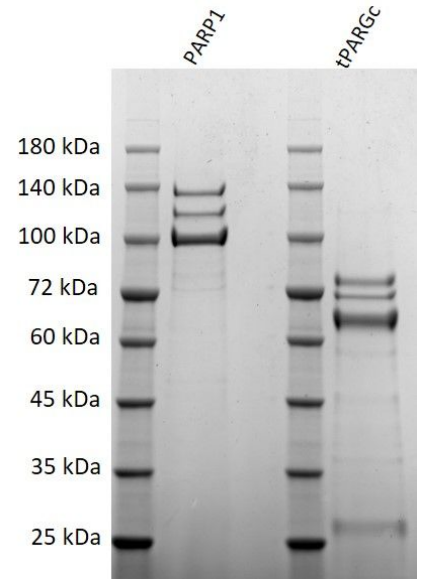

Figure S1. Coomassie stain of purified PARP1 (left) and tPARG (right).

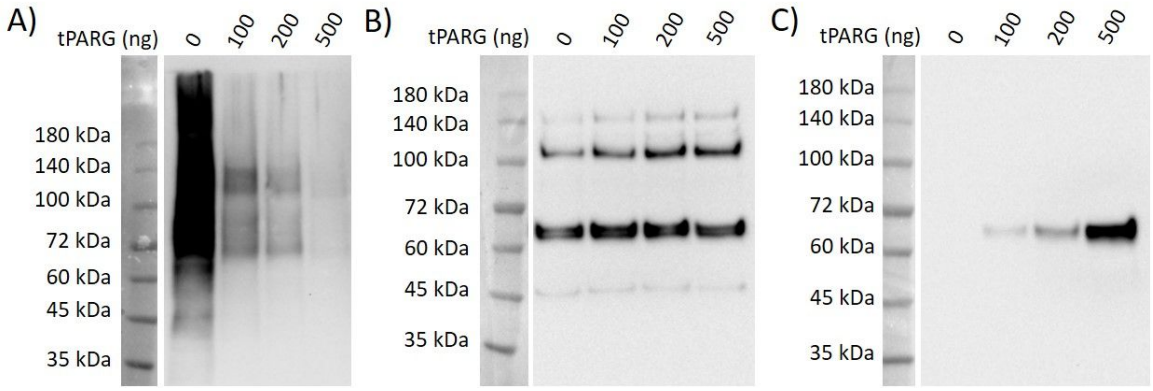

Figure S2. Immunoblots for enzymatic activity of tPARG. 0, 100, 200, or 500 ng of tPARG was added to 300 ng of PARP1 automodified with NAD^+ and incubated for 30 minutes at room temperature. Remaining PARylated PARP1 was detected using (A) Fc-WWE. Loading controls were detected by (B) anti-PARP1 and (C) anti-PARG antibodies. The observed bands between 45 and 72 kDa in (B) were proteolyzed PARP1 formed during auto-modification reactions.

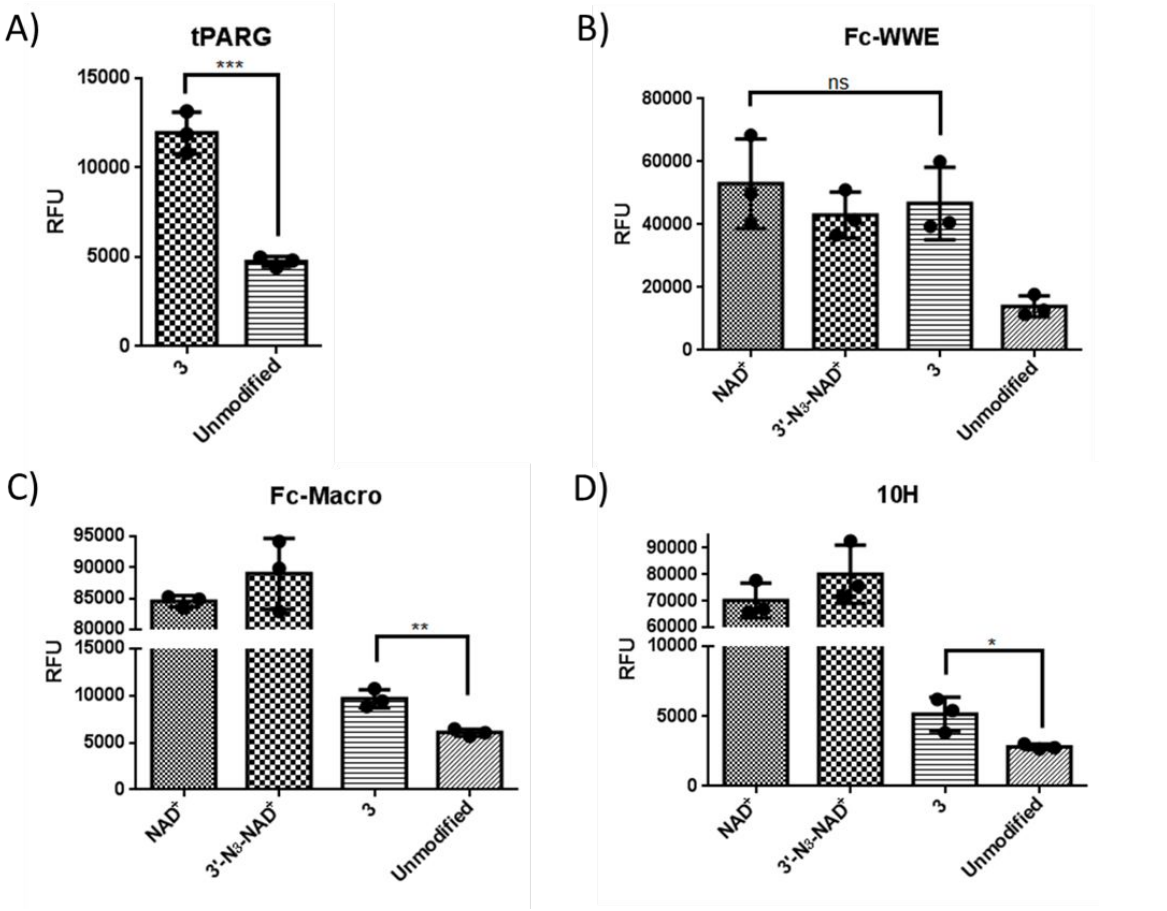

Figure S3. Binding of model interacting proteins for unmodified PARP1 and automodified PARP1 by NAD^+ and NAD^+ analogues. Unmodified PARP1 and automodified PARP1 by NAD^+, 3′-N_3-NAD^+, or **3** were coated on 96-well ELISA plates for binding analysis with (A) tPARG, (B) Fc-WWE, (C) Fc-Macro, and (D) antibody 10H. NAD^+ and 3′-N_3-NAD^+ were excluded from binding analysis with tPARG due to PARG degrading activity with PARylated PARP1 derived from these two compounds. ns: not significant, $*P < 0.05$, $**P < 0.01$, $***P < 0.001$ by one-tailed unpaired *t*-test. Error bars represent standard deviation of three replicates. RFU: relative fluorescence unit.

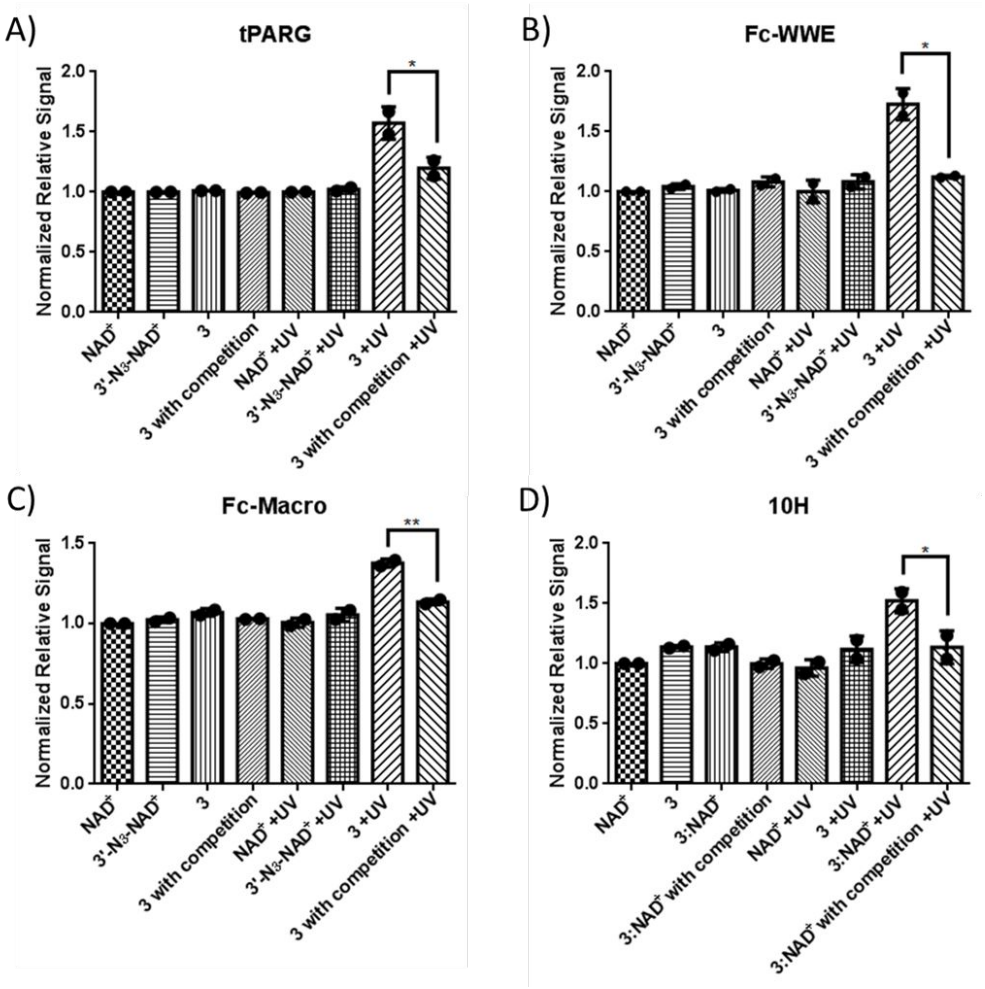

Figure S4. Relative densitometric analysis of photocrosslinking levels of automodified PARP1 with model interacting proteins. PARP1 PARylated by NAD^+, 3′-N_3-NAD^+, **3**, or mixture of **3**:NAD^+ was incubated with (A) tPARG, (B) Fc-WWE, (C) Fc-Macro, and (D) antibody 10H in the absence or presence of 365-nm UV irradiation and automodified PARP1 by NAD^+ for competition, followed by immunoblot analysis using antibodies specific for model interacting proteins. Regions above expected size of the binding proteins were quantified and normalized to the density in the lane with NAD^+ and without UV for the respective blots in Figure 3. $*P < 0.05$ and $**P < 0.01$ by one-tailed unpaired *t*-test. Error bars represent standard deviation of two replicates.

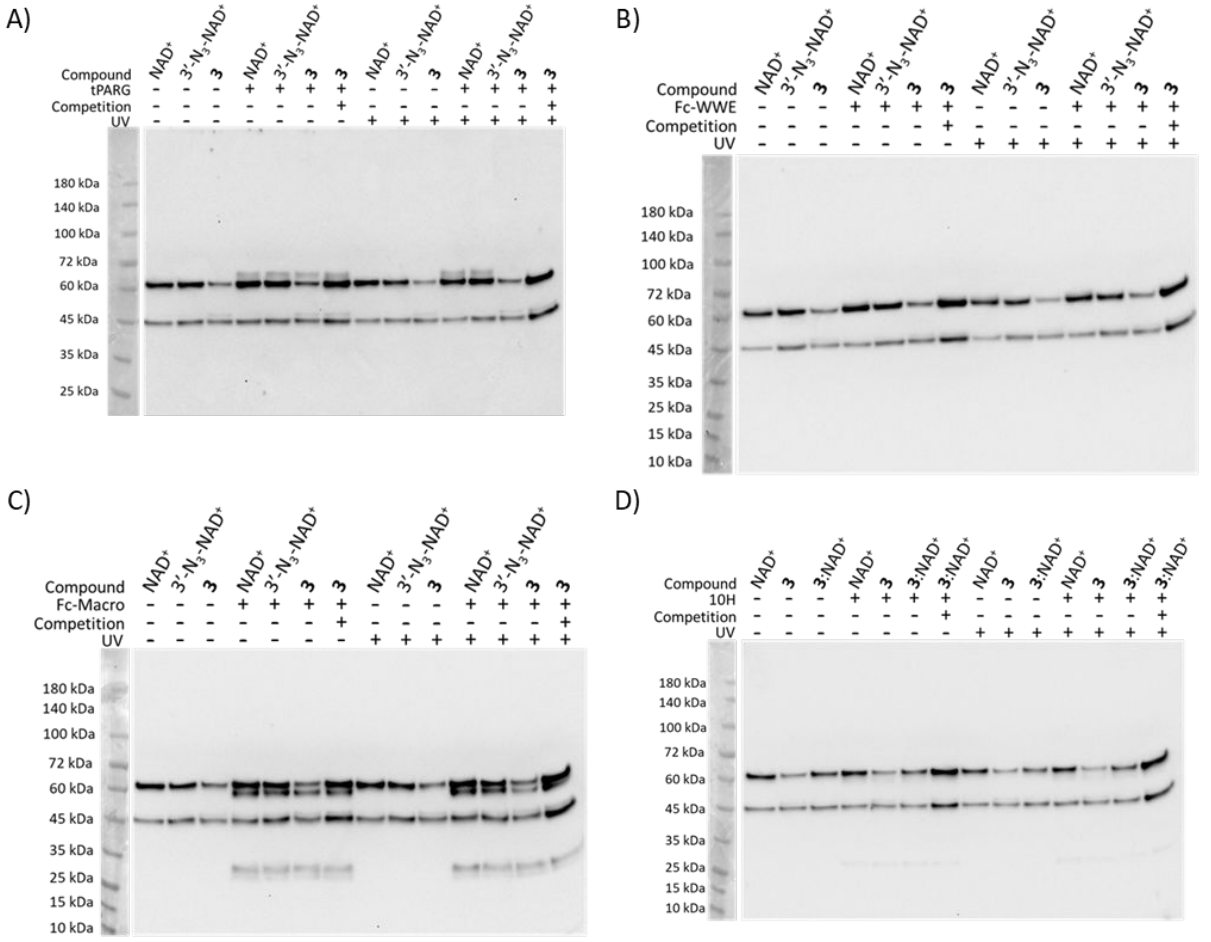

Figure S5. Full-sized anti-His_6 blots for Figure 3. PARP1 PARylated by NAD^+, 3′-N_3-NAD^+, **3**, or a mixture of **3**:NAD^+ at a 1:1 molar ratio was incubated with (A) tPARG, (B) Fc-WWE, (C) Fc-Macro, and (D) antibody 10H in the absence or presence of 365-nm UV irradiation and automodified PARP1 by NAD^+ for binding competition. The PARP1 loading controls were detected using an anti-His_6 antibody. The observed bands between 45 and 72 kDa were proteolyzed PARP1 formed during auto-modification reactions.

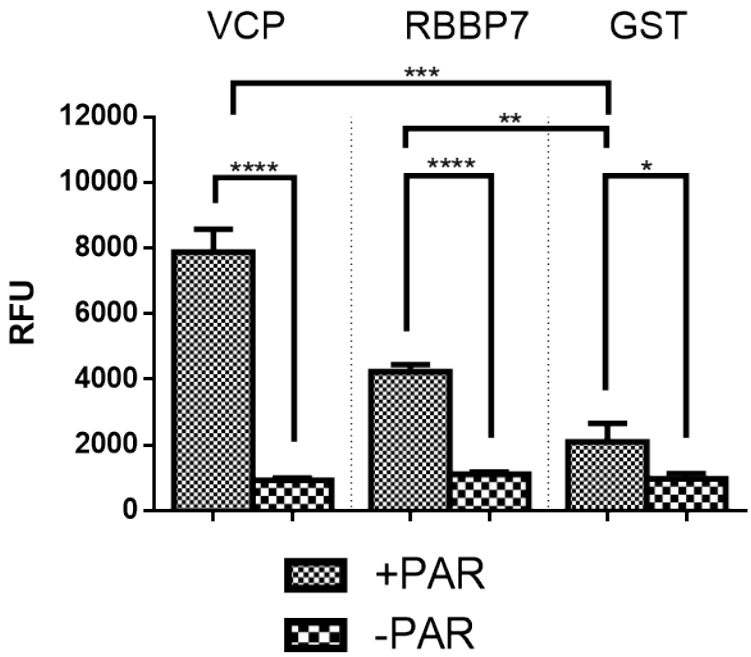

Figure S6. Binding of GST-VCP and GST-RBBP7 to PAR. Sandwich ELISA analyses were performed by coating GST-VCP, GST-RBBP7, and GST onto plates to capture PAR and detecting with the 10H anti-PAR monoclonal antibody and anti-mouse HRP conjugated secondary antibody. *P < 0.05, **P < 0.01, ***P < 0.001, and ****P < 0.0001 by one-tailed unpaired *t*-test. Error bars represent standard deviation of three replicates.

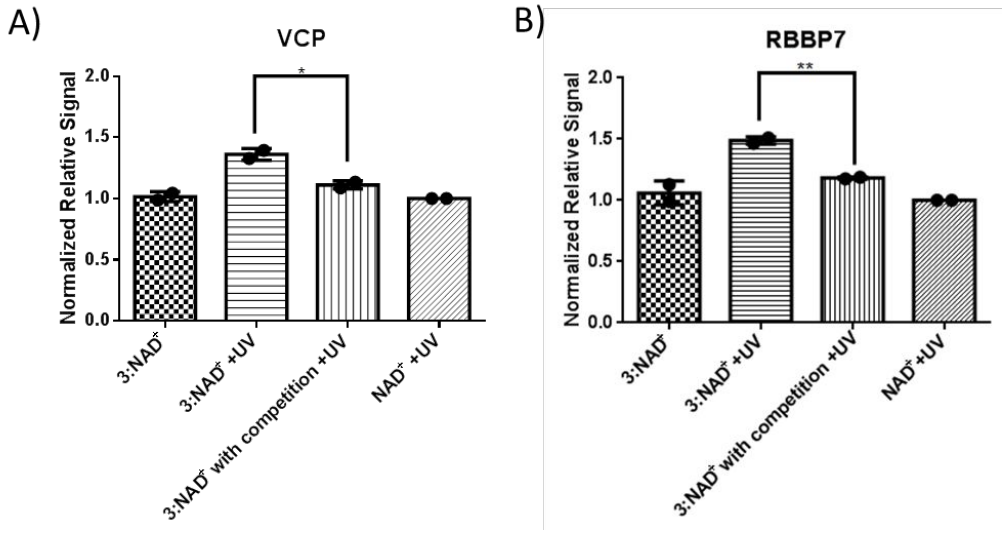

Figure S7. Relative densitometric analysis of photocrosslinking levels of automodified PARP1 with the identified interacting proteins. PARP1 PARylated by NAD^+ or mixture of **3**:NAD^+ was incubated with (A) GST-VCP and (B) GST-RBBP7 without and with 365-nm UV and NAD^+-modified PARP1 for competition, followed by immunoblot analysis using the anti-GST antibody. Regions above expected size of the binding proteins were quantified and normalized to the density in the lane with NAD^+ and UV for the respective blots in Figure 4. $^*P < 0.05$ and $^{**}P < 0.01$ by one-tailed unpaired *t*-test. Error bars represent standard deviation of two replicates.

Supplemental Methods

Purification of human PARP1. Full-length human PARP1 with a C-terminal His_6-tag was expressed in *Escherichia coli* as described in a previous study[1]. BL21(DE3) cells were transformed with plasmid containing human PARP1-His_6 and grown overnight in a temperature-controlled shaker at 37°C at 250 rpm. Each overnight culture was inoculated into 1 L of LB broth with 50 μg mL^{-1} kanamycin and grown to $OD_{600\ nm}$ = 0.8 in a temperature-controlled shaker at 37°C at 250 rpm. Cultures were induced with 500 μM isopropyl β-D-1-thiogalactopyranoside (IPTG) and grown overnight at 16°C at 250 rpm. Cells were harvested by centrifugation for 30 minutes at 2,700×g. Cell pellets were resuspended in 30 mL of lysis buffer (20 mM Tris-HCl pH 7.5, 500 mM NaCl, 1 mM beta-mercaptoethanol (β-ME), 0.2% Nonidet P-40 (v/v), and 0.2% Tween-20 (v/v) with 1 mg mL^{-1} lysozyme (VWR: VWRV0663), and 1 mM phenylmethylsulfonyl fluoride (PMSF) (Chem-Impex: 00632). Cells were lysed by running cells through a French Press (Glen Mills) at 25,000 psi three times.

Cell debris was spun down at 27,000×g. 1 mL Ni-NTA agarose resin (ThermoFisher: 88221) gravity flow columns were equilibrated with 15 CV of equilibrium buffer (20 mM Tris-HCl pH 7.5, 500 mM NaCl, 20 mM imidazole, 1 mM β-ME, and 1 mM PMSF) before adding cell lysates. The column was then washed with 15 CV of equilibrium buffer. Bound proteins were eluted with 15 CV of elution buffer (20 mM Tris-HCl pH 7.5, 500 mM NaCl, 400 mM imidazole, and 1 mM β-ME). Proteins were concentrated with 30 kDa MWCO Ultra-15 Centrifugal Filter Units (Millipore: UFC903024) before dilution of the samples in storage buffer (100 mM Tris-HCl pH 7.5, 150 mM NaCl, 0.1 mM EDTA, and 1 mM β-ME) at 1:10 before loading with a syringe onto a 5-mL heparin column (GE Life Sciences: 17040601) equilibrated with heparin binding buffer (50 mM Tris-HCl pH 7.5, 250 mM NaCl, 0.1 mM EDTA, and 1 mM β-ME). The column was connected to an AKTA FPLC Pure (GE Healthcare) and weakly bound proteins were washed off with heparin binding buffer. Elution with heparin elution buffer (50 mM Tris-HCl pH 7.5, 1000 mM NaCl, 0.1 mM EDTA, and 1 mM β-ME) was done with a gradient of 20% to 80% over 3 CVs and fractions with protein were collected. Collected fractions were concentrated and loaded onto a Superdex 75 Increase 10/300 column (GE Healthcare: 29148721) pre-equilibrated with storage buffer. An isocratic gradient with a flow rate of 0.5 mL min^{-1} was used to separate 0.5 mL fractions, which were run on a PAGE gel to identify fractions containing the desired protein. Fractions were combined and concentrated by centrifugal filter units. Protein was examined by SDS-PAGE and UV-absorption spectrophotometry, analyzing the wavelength at 280 nm and using an extinction coefficient of 1.05.

Purification of truncated PARG (tPARG). cDNA encoding human PARG was purchased from GE Dharmacon (MHS6278-202759481), and primers were designed to amplify a truncated PARG containing the catalytic domain (amino acids 448-976) for insertion into the pET28a (+) vector[2-4]. Plasmids containing tPARG were transformed into BL21(DE3) for expression and purification.

Purification of tPARG was performed as described previously with modifications[2]. 5 mL of LB broth with 50 μg mL^{-1} kanamycin were inoculated and grown overnight in a temperature-controlled shaker at 37°C at 250 rpm. Each overnight culture was inoculated into 1 L of LB broth with 50 μg mL^{-1} kanamycin and grown to $OD_{600\ nm}$ = 0.6 in a temperature-controlled shaker at 37°C at 250 rpm. Cultures were induced using a 500 mM stock of IPTG to a final concentration of 100 μM and grown overnight at 18°C at 250 rpm. Cells were harvested by centrifugation for 30 minutes at 2,700×g. Cell pellets were then resuspended in 30 mL of

equilibrium buffer, and cells were lysed by running cells through a French Press at 25,000 psi three times. Cell debris was spun down at 27,000×g. 1 mL Ni-NTA agarose resin gravity flow columns were equilibrated with 15 CVs of equilibrium buffer (20 mM Tris-HCl pH 7.5, 500 mM NaCl, 20 mM imidazole, 1 mM β-ME, and 1 mM PMSF) before adding cell lysates. The column was then washed with 15 CVs of equilibrium buffer. An additional wash with 15 mL of wash buffer (20 mM Tris-HCl pH 7.5, 500 mM NaCl, 30 mM imidazole, and 1 mM β-ME) was included afterwards. Bound proteins were eluted with 15 CVs of elution buffer (20 mM Tris-HCl pH 7.5, 500 mM NaCl, 400 mM imidazole, and 1 mM β-ME). Proteins were concentrated with 30 kDa MWCO Ultra-15 Centrifugal Filter Units, and the buffer was exchanged into storage buffer (20 mM Tris-HCl pH 7.5, 300 mM NaCl, 1 mM β-ME, and 10% (v/v) glycerol). Protein was examined by SDS-PAGE and UV-absorption spectrophotometry, analyzing the wavelength at 280 nm and using an extinction coefficient of 1.3.

Copper(I)-catalyzed alkyne-azide cycloaddition (CuAAC). Automodified PARP1 was conjugated to alkyne-biotin by CuAAC by adding 3× CuAAC buffer (4.5 mM tris(3-hydroxypropyltriazolylmethyl)amine (THPTA) (Click Chemistry Tools: 1010), 2.25 mM $CuSO_4$, 900 μM biotin-PEG4-alkyne (Sigma-Aldrich: 764213), 22.5 mM sodium ascorbate) to samples and incubating for 1 hour at room temperature.

PARP1 automodification activity with NAD^+ analogues. PARP1 automodification was performed in PARP reaction buffer (100 mM Tris-HCl pH 8.0, 10 mM $MgCl_2$, 50 mM NaCl, 1 mM DTT, and 100 ng μL^{-1} activated DNA (Sigma-Aldrich: GE27-4575-01)) for 30 minutes at 30°C. 3 μM of PARP1 was added to reaction buffer with 400 μM of NAD^+ analogues. Olaparib (Selleckchem: S1060) was used at a concentration of 100 μM for conditions with olaparib. All reactions were stopped by the additions of 100 μM of olaparib. Automodified PARP1 was conjugated to alkyne-biotin and run on precast PAGE gels (GenScript: M42015) for immunoblot detection. Proteins were transferred onto PVDF membranes (BioRad: 1620177) and blocked with 3% BSA (w/v) in PBS with 0.1% Tween-20 (v/v) (PBST) for 1 hour. After washing, detection was done with 1:200 streptavidin-HRP conjugate (R&D Systems: DY998) in PBST. Blots were imaged using SuperSignal West Pico PLUS Chemiluminescent Substrate (ThermoFisher: 34580) and ChemiDoc Touch Gel Imaging System (Bio-Rad: 1708370). Densitometric analysis was done by measuring the levels of PARylation signals in each lane using ImageJ (https://imagej.nih.gov/ij/index.html)[5] and normalizing to the signals from 3′-N_3-NAD^+. Loading controls were detected by blocking in 5% non-fat milk (w/v) (BioRad: 170-6404) and using 1:3000 anti-His_6 antibody (ThermoFisher: MA1-21315) and 1:3000 anti-mouse secondary antibody conjugated to HRP (ThermoFisher: G-21040) for primary and secondary antibody incubations, respectively.

Kinetic analysis for PARP1 automodifications with NAD^+ and NAD^+ analogues. Standards of NAD^+ and NAD^+ analogues were run at 0 μM, 20 μM, 50 μM, 100 μM, 200 μM, 400 μM, and 600 μM. ADPr was purchased from Sigma-Aldrich (A0752) and standards were run at 10 μM, 20 μM, and 50 μM. ADPr analogues were derived from cleavage of NAD^+ analogues using 7 N ammonia in overnight reactions and peaks were identified by mass spectrometric analysis. Standards for the ADPr analogues were run at similar concentrations to ADPr. Standard curves were generated by correlating the integrated peak areas to the corresponding concentration of the standards for each compound.

Automodifications of PARP1 were carried out in 50 μL reactions per condition and time point. 0.9 μM of PARP1 was added to PARP reaction buffer (100 mM Tris-HCl pH 8.0, 10 mM $MgCl_2$ 50 mM NaCl, 1 mM DTT, and 100 ng μL^{-1} activated DNA) and preincubated for 15

minutes to activate PARP1. NAD^+ or NAD^+ analogues were added to initiate the reactions at final concentrations of 20 μM, 50 μM, 100 μM, 200 μM, 400 μM, or 600 μM and incubated at 30°C. Three timepoints were taken at 0, 3, and 6 minutes for separation by HPLC. Reactions were quenched with additions of 50 μL ice-cold 20% trichloroacetic acid (w/v) and injected on a Waters HPLC for separation and detection at 260 nm. The concentrations of each compound of interest were calculated by integrating the peak areas and conversion to concentrations using the standard curves for the respective compounds.

End point assays were run to estimate the maximum k_{cat} for PARP1 NADase activity with **3** and 3′-N_3-NAD^+. For **3**, two time points at 0 and 180 minutes were taken for a reaction of 750 μM of **3** with 0.9 μM of PARP1. For 3′-N_3-NAD^+, two time points at 0 and 120 minutes were taken for a reaction of 600 μM of 3′-N_3-NAD^+ with 3 μM PARP1. The amount of ADPr analogue derived from each compound was compared to a standard curve to determine the maximum rate of PARP1 NADase activity with each compound.

Separations for reaction mixtures were done using a Kinetex C18 column (5 μm, 100 Å, 150 × 10.0 mm, Phenomenex Inc: 00F-4601-N0). The gradient program consisted of running water containing 0.1% formic acid (v/v) (A) and acetonitrile with 0.1% formic acid (v/v) (B) at 2 mL min^{-1} at a gradient of 0–8 min 0% B; 8–13 min 0–25% B; 13–18 min 25–40% B; 18–20 min 40–80% B; 20–21 min 80–0% B; 21–24 min 0% B.

Separations for **3**-derived reaction mixtures were done using a Luna C18 column (5 μm, 100 Å, 150 × 4.6 mm, Phenomenex Inc: 00F-4252-E0). The gradient program consisted of running water containing 0.1% formic acid (v/v) (A) and acetonitrile with 0.1% formic acid (v/v) (B) at 2 mL min^{-1} at a gradient of 0–2 min 0–4% B; 2–4 min 4–10% B; 4–6 min 10–20% B; 6–12 min 20–50% B; 12–14 min 50% B; 14–16 min 50–0% B.

Separations for ADPr of **3-**derived reaction mixtures were done using the Luna C18 column with water containing 0.1% formic acid (v/v) (A) and acetonitrile with 0.1% trimethylamine (v/v) (C) using a gradient program consisting of 0–8 min 0% C; 8–13 min 0–2.5% C; 13–18 min 2.5–30% C; 18–24 min 30–40% C; 24–29 min 40% C; 29–30 min 40–0% C; 30–32 min 0% C at 1 mL min^{-1} for 0-24 min and then 1.5 mL min^{-1} for 24-30 min.

The transferase activities of PARP1 with NAD^+ and NAD^+ analogues were determined by the rates of decrease of the peak areas for the respective compounds. The NADase activities of PARP1 were determined by the rates of formation of the ADPr derived from their respective compounds. Kinetic parameters were determined by analysis using GraphPad Prism.

PARG-mediated degradation of PARylation. PARP1 automodification was performed in PARP reaction buffer with 3 μM of PARP1 and 200 μM of NAD^+ for 30 minutes at room temperature and stopped with 100 μM of olaparib. Various amounts of tPARG were added to 300 ng of automodified PARP1 with NAD^+ in PBS in 12 μL for 30 minutes at room temperature. Reactions examined by immunoblot detection using 1:5000 Fc-WWE (Millipore: MABE1031) as the primary antibody for 1 hour followed by anti-rabbit secondary antibody (System Biosciences) at 1:3000 in PBS with 0.05% (v/v) Tween-20 with 1% (w/v) milk for 1-hour incubation. Detection was done as indicated above.

Chemical Synthesis and Characterization of NAD^+ analogues 1-3.

General Materials and Methods for Synthesis of Compounds.

^1H NMR spectra were recorded on an Oxford AM-400 spectrometer for solution in $CDCl_3$, CD_3OD or D_2O. Coupling constants *J* are shown in Hz. ^{13}C NMR spectra were recorded on an Oxford AM-400 spectrophotometer (100 MHz) with complete proton decoupling spectrophotometer ($CDCl_3$: 77.0 ppm). Flash column chromatography was performed using 230-

400 mesh silica gel (Sigma-Aldrich, St. Louis, MO). For thin-layer chromatography (TLC), silica gel plates (Sigma-Aldrich GF254) were used. HPLC was performed on a Waters 2487 series with C18 Kinetex column (5 μm, 100 Å, 150×10.0 mm, from Phenomenex Inc, Torrance, CA). All other reagents were purchased from readily available commercial sources and used without further purification.

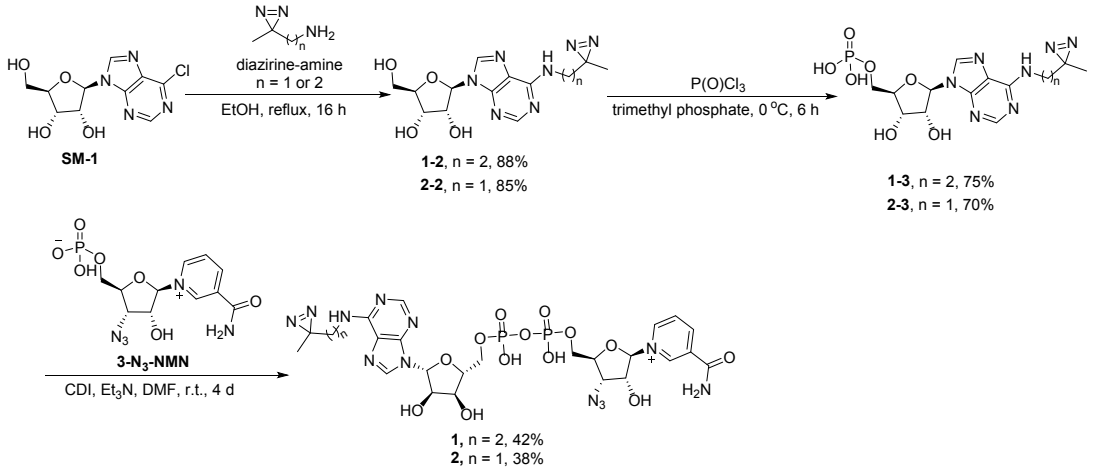

Scheme S1. Chemical synthesis of **1** and **2.**

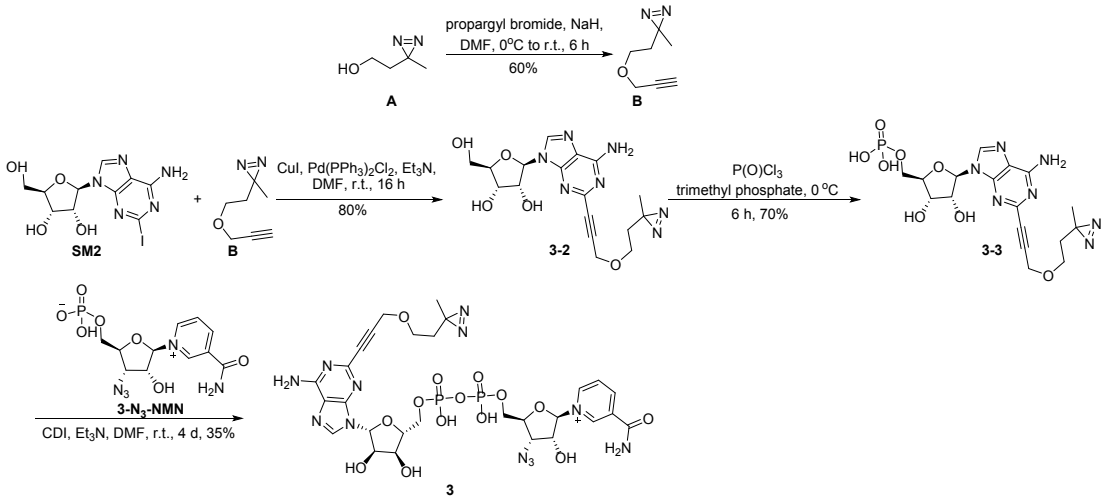

Scheme S2. Chemical synthesis of **3.**

*General procedure for the synthesis of compound **1-2** or **2-2***: To a solution of 6-chloropurine riboside (**SM1**) (57 mg, 0.2 mmol) in EtOH (4.0 mL) were added corresponding diazirine-amine (0.22 mmol, 1.1 eq) and DIPEA (105 μL, 0.6 mmol, 3 eq) at room temperature. Then the resulting mixture was heated to reflux until the reactions completed (monitoring by TLC). Then the solvent was removed under reduced pressure and the residue was purified by a flash column chromatography to afford the desired products **1-2** or **2-2**.

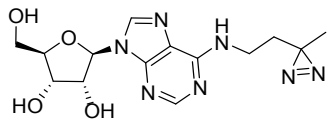

1-2

(2*R*,3*S*,4*R*,5*R*)-2-(hydroxymethyl)-5-(6-((2-(3-methyl-3*H*-diazirin-3-yl)ethyl)amino)-9*H*-purin-9-yl)tetrahydrofuran-3,4-diol (1-2). A colorless solid, 61 mg, 88% yield; ^{1}H NMR (400 MHz, CD_3OD): δ 1.07 (s, 3H, CH_3), 1.73 (t, 2H, J = 7.2 Hz, CH_2), 3.55 (br, 2H, CH_2), 3.75 (dd, 1H, J = 12.4, 2.8 Hz, CH_2), 3.89 (dd, 1H, J = 12.4, 2.4 Hz, CH_2), 4.17 (q, 1H, J = 2.8 Hz, CH), 4.32 (dd, 1H, J = 5.2, 2.8 Hz, CH), 4.75 (dd, 1H, J = 6.4, 5.2 Hz, CH), 5.95 (d, 1H, J = 6.8 Hz, CH), 8.23 (s, 1H, ArH), 8.26 (s, 1H, ArH); ^{13}C NMR (100 MHz, CD_3OD): δ 19.9, 25.3, 35.1, 36.8, 63.5, 72.7, 75.4, 88.2, 91.3, 121.6, 141.6, 149.1, 153.4, 156.2； MS (ESI) *m/z*: 350.1 $(M+H)^+$.

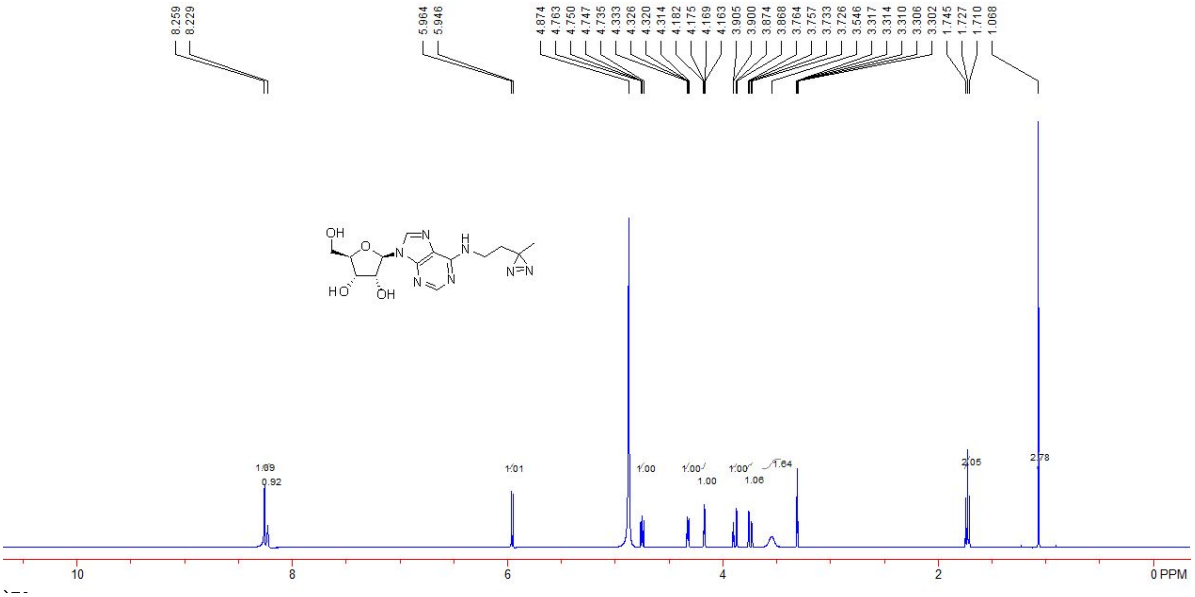

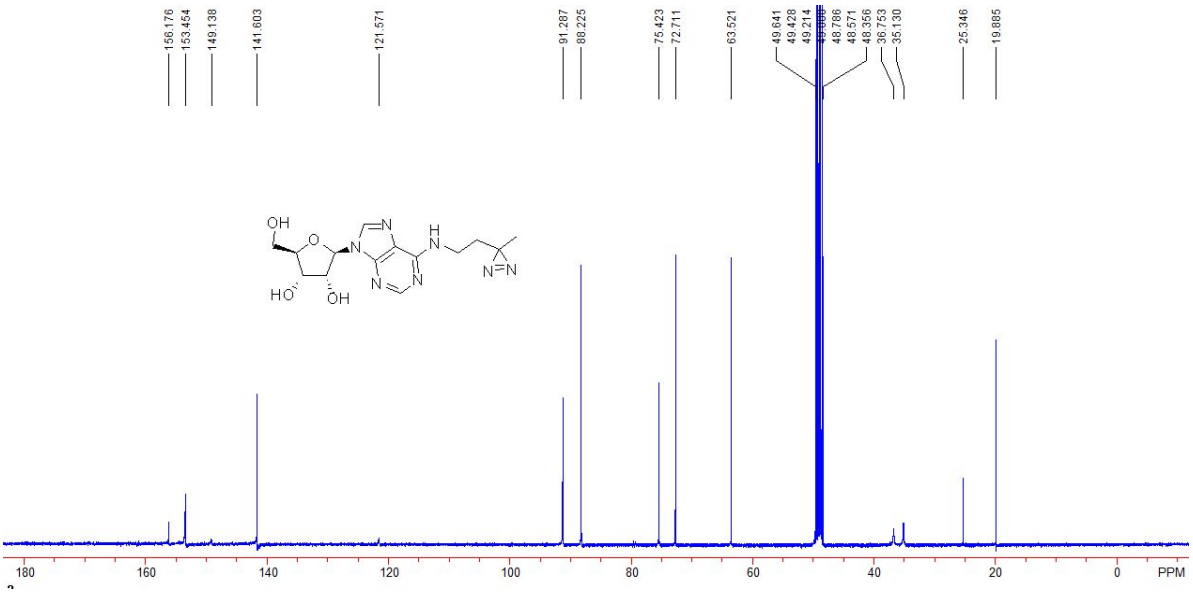

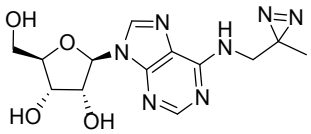

2-2

(2*R*,3*S*,4*R*,5*R*)-2-(hydroxymethyl)-5-(6-(((3-methyl-3*H*-diazirin-3-yl)methyl)amino)-9*H*-purin-9-yl)tetrahydrofuran-3,4-diol (2-2). A colorless solid, 60 mg, 85% yield; ^{1}H NMR (400 MHz, CD_3OD): δ 1.10 (s, 3H, CH_3), 3.63 (br, 2H, CH_2), 3.75 (dd, 1H, J = 12.4, 2.4 Hz, CH_2), 3.89 (dd, 1H, J = 12.4, 2.0 Hz, CH_2), 4.16-4.18 (m, 1H, CH), 4.33 (dd, 1H, J = 5.2, 2.0 Hz, CH), 4.75 (dd, 1H, J = 6.4, 5.2 Hz, CH), 5.96 (d, 1H, J = 6.4 Hz, CH), 8.27 (s, 2H, ArH); ^{13}C NMR (100 MHz, CD_3OD): δ 18.1, 26.8, 44.1, 63.5, 72.7, 75.4, 88.2, 91.3, 121.5, 141.8, 149.4, 153.3, 156.1; MS (ESI) *m/z*: 336.0 $(M+H)^+$.

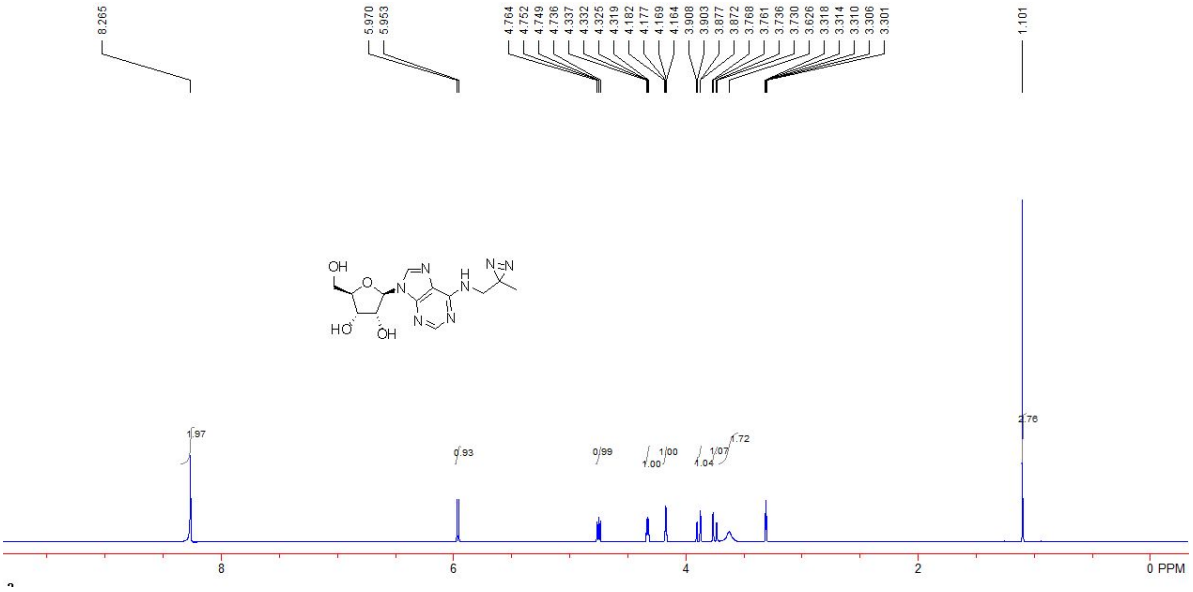

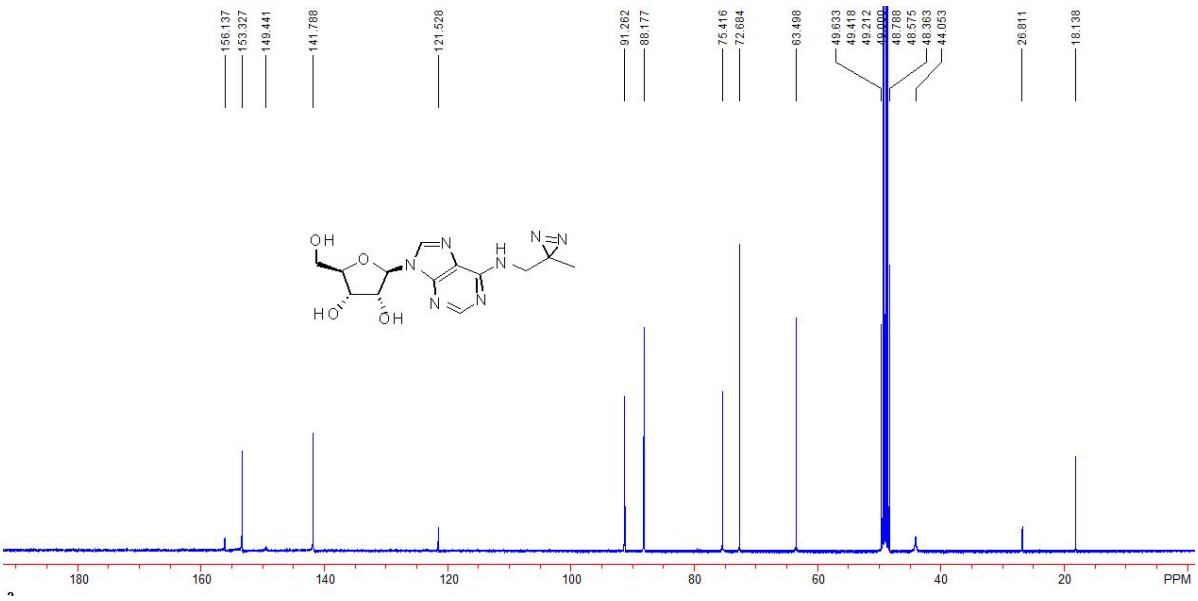

*General procedure for the synthesis of compound **B***: To a stirred solution of 2-(3-methyl-3H-diazirin-3-yl)ethan-1-ol **A** (100 mg, 1.0 mmol) in anhydrous THF (5 mL) was added NaH (48 mg, 1.2 mmol, 1.2 eq, 60% dispersion in mineral oil) at 0°C, followed by the addition of propargyl bromide (177 mg, 1.5 mmol, 1.5 eq) at the same temperature. Then, the reaction mixture was allowed to warm to room temperature. After stirring at this temperature for 6 hours, the reaction mixture was quenched with saturated aqueous NH_4Cl (10 mL) and extracted with EtOAc (3×25 mL). The combined organic layers were washed by water (3×25 mL), dried over anhydrous Na_2SO_4, filtered and concentrated and purified by a flash column chromatography on silica gel to afford the compound **B** (83 mg, 60%) as a colorless oil.

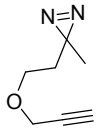

B

3-methyl-3-(2-(prop-2-yn-1-yloxy)ethyl)-3H-diazirine. ^{1}H NMR (400 MHz, $CDCl_3$): δ 1.06 (s, 3H, CH_3), 1.63 (t, 2H, J = 6.4 Hz, CH_2), 2.43 (t, 1H, J = 2.4 Hz, CH), 3.42 (t, 2H, J = 6.4 Hz, CH_2), 4.13 (d, 2H, J = 2.4 Hz, CH_2); ^{13}C NMR (100 MHz, $CDCl_3$): δ 20.1, 24.3, 34.5, 58.2, 64.8, 74.6, 79.4.

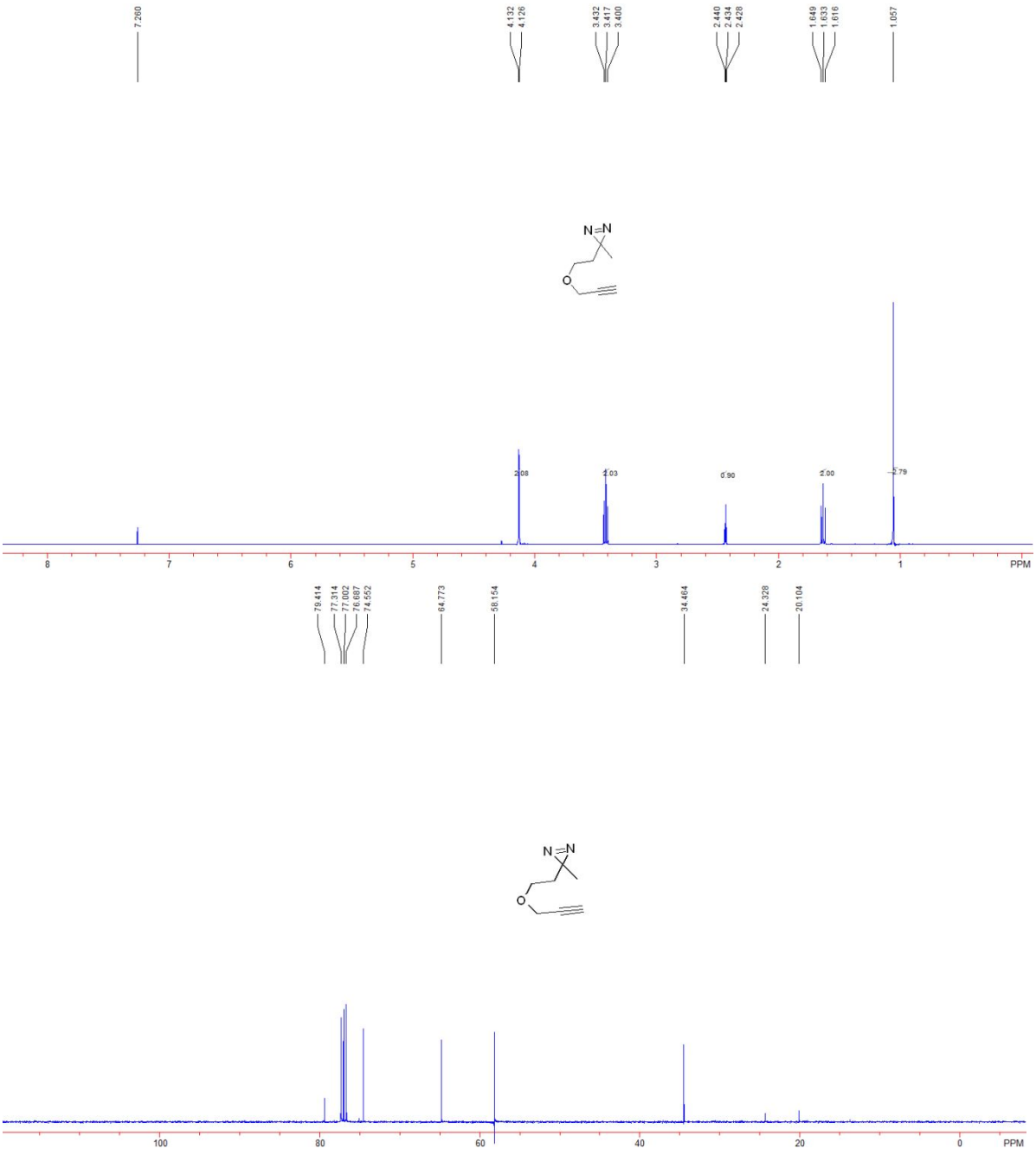

*General procedure for the synthesis of compound **3-2***: Under an argon atmosphere, to a stirred solution of 2-iodoadenosine (**SM2)** (59 mg, 0.15 mmol) in dried DMF (2 mL) were added CuI (6 mg, 0.030 mmol, 0.2 eq), $Pd(PPh_3)_2Cl_2$ (11 mg, 0.015 mmol, 0.1 eq), 3-methyl-3-(2-(prop-2-yn-1-yloxy)ethyl)-3H-diazirine (**B**) (42 mg, 0.30 mmol, 2 eq) and triethylamine (63 µL, 0.45 mmol. 3 eq) at room temperature. The reaction mixture was stirred without light at room temperature for 24 hours. The reaction was then concentrated *in vacuo* and the crude product was purified via preparative HPLC (semipreparative C18 Kinetex column (5 µm, 100 Å, 150×10.0 mm) (mobile phase A: 0.1% formic acid (aq), mobile B: 0.1% formic acid in acetonitrile; flow rate = 2.0 mL min^{-1}; 0-2 min: 0-4% B, 2-4 min: 4-10% B; 4-6 min: 10-20% B; 6-12 min: 20-50% B; 12-17

min: 50-100% B; 17-20 min: 100-0% B). Fractions containing the desired product were concentrated and lyophilized to yield the desired products **3-2** (48 mg, 80% yield) as a colorless solid.

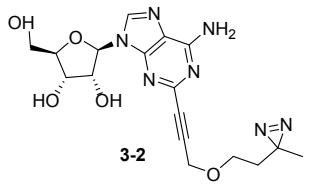

3-2

(2R,3R,4S,5R)-2-(6-amino-2-(3-(2-(3-methyl-3H-diazirin-3-yl)ethoxy)prop-1-yn-1-yl)-9H-purin-9-yl)-5-(hydroxymethyl)tetrahydrofuran-3,4-diol (3-2). ^{1}H NMR (400 MHz, CD_3OD): δ 1.05 (s, 3H, CH_3), 1.61 (t, 2H, J = 6.0 Hz, CH_2), 3.56 (t, 2H, J = 6.0 Hz, CH_2), 3.76 (dd, 1H, J = 12.4, 2.4 Hz, CH_2), 3.91 (dd, 1H, J = 12.4, 2.4 Hz, CH_2), 4.17 (q, 1H, J = 2.4 Hz, CH), 4.33 (dd, 1H, J = 5.2, 2.4 Hz, CH), 4.39 (s, 2H, CH_2), 4.72 (t, 1H, J = 5.6 Hz, CH), 5.95 (d, 1H, J = 6.4 Hz, CH), 8.35 (s, 1H, ArH); ^{13}C NMR (100 MHz, CD_3OD): δ 20.1, 25.2, 35.6, 59.1, 63.4, 66.3, 72.5, 75.4, 83.0, 85.7, 88.1, 91.3, 120.7, 142.8, 146.7, 150.1, 157.3; MS (ESI) *m/z*: 404.1 $(M+H)^+$.

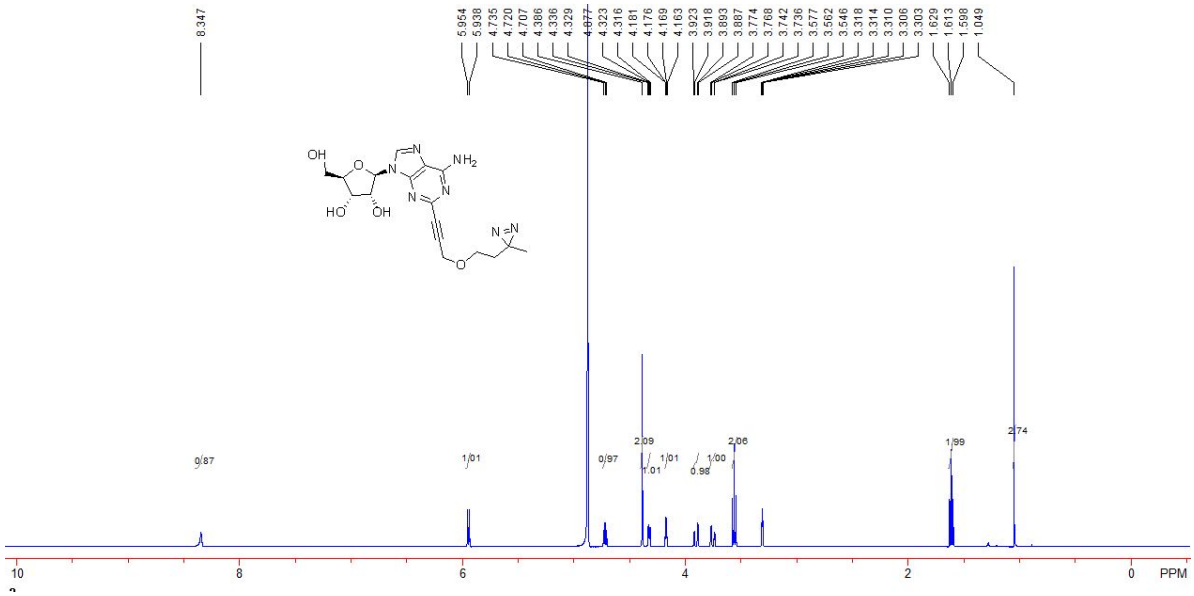

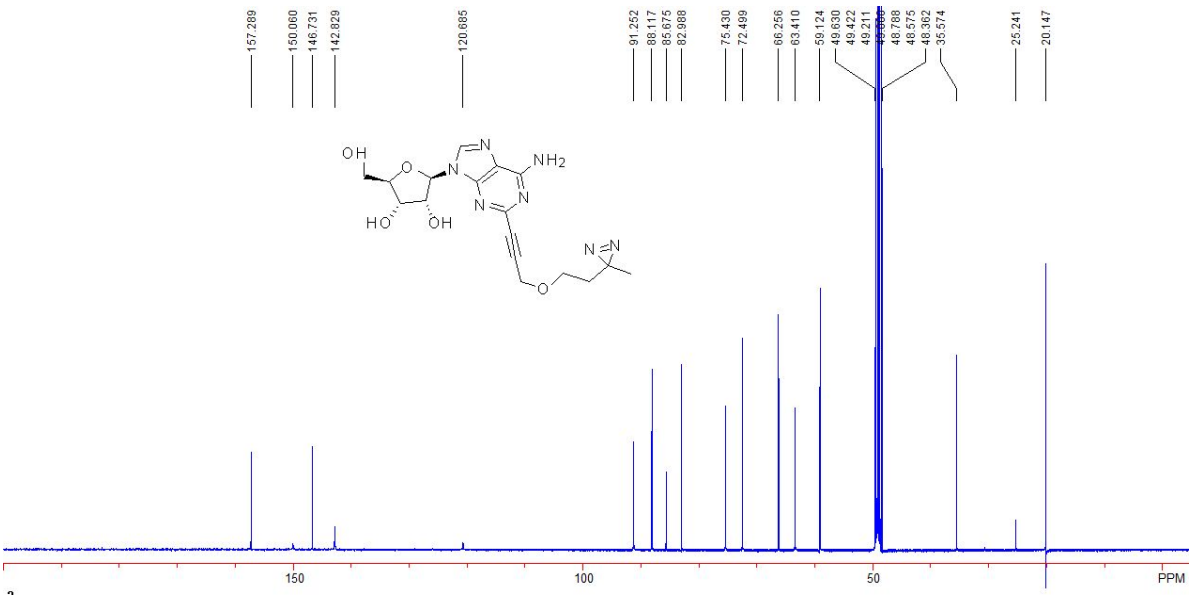
157.289
150.060
146.731
142.829
120.685
91.252
88.117
85.675
82.988
75.430
72.499
66.256
63.410
59.124
49.630
49.422
49.211
48.788
48.575
48.362
35.574
25.241
20.147
OH
HO
OH
NH2
N
O
150
100
50
PPM

*General procedure for the synthesis of compound **1-3, 2-3 or 3-3***: To a stirred solution of compound **1-2**, **2-2**, or **3-2** (0.15 mmol) in trimethylphosphate (2 mL) was added $P(O)Cl_3$ (42 µL, 0.45 mmol, 3 eq) at 0°C and the resulting mixture was stirred at 0°C for 6 hours. A few drops H_2O was then added to quench the reaction. The reaction was then concentrated *in vacuo* and the crude product was purified via preparative HPLC (semipreparative C18 Kinetex column (5 µm, 100 Å, 150×10.0 mm) (mobile phase A: 0.1% formic acid (aq), mobile B: 0.1% formic acid in acetonitrile; flow rate = 2.0 mL min^{-1}; 0-2 min: 0-4% B, 2-4 min: 4-10% B; 4-8 min: 10-20% B; 8-9 min: 20% B; 9-12 min: 20-50% B; 12-14 min: 50-0% B). Fractions containing the desired product were concentrated and lyophilized to yield the desired products ***1-3, 2-3 or 3-3***.

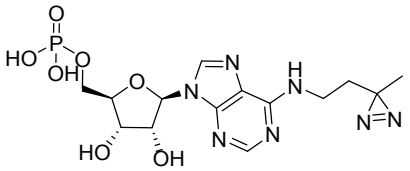

1-3

((2*R*,3*S*,4*R*,5*R*)-3,4-dihydroxy-5-(6-((2-(3-methyl-3*H*-diazirin-3-yl)ethyl)amino)-9*H*-purin-9-yl)tetrahydrofuran-2-yl)methyl dihydrogen phosphate (1-3). A colorless solid, 48 mg, 75% yield; ^{1}H NMR (400 MHz, D_2O): δ 1.06 (s, 3H, CH_3), 1.86 (br, 2H, CH_2), 3.51 (br, 2H, CH_2), 4.08-4.19 (m, 2H, CH_2), 4.37-4.39 (m, 1H, CH), 4.49 (t, 1H, J = 4.8 Hz, CH), 4.73 (t, 1H, J = 5.2 Hz, CH), 6.15 (d, 1H, J = 6.0 Hz, CH), 8.38 (s, 1H, ArH), 8.58 (s, 1H, ArH); ^{13}C NMR (100 MHz, D_2O): δ 18.6, 24.8, 32.1, 37.2, 64.2 (d, J = 4.7 Hz), 70.2, 74.6, 84.2 (d, J = 8.7 Hz), 87.8, 118.8, 141.5, 145.5, 146.8, 149.2; ^{31}P NMR (162 MHz, D_2O): δ 0.13; MS (ESI) *m/z*: 430.1 $(M+H)^+$.

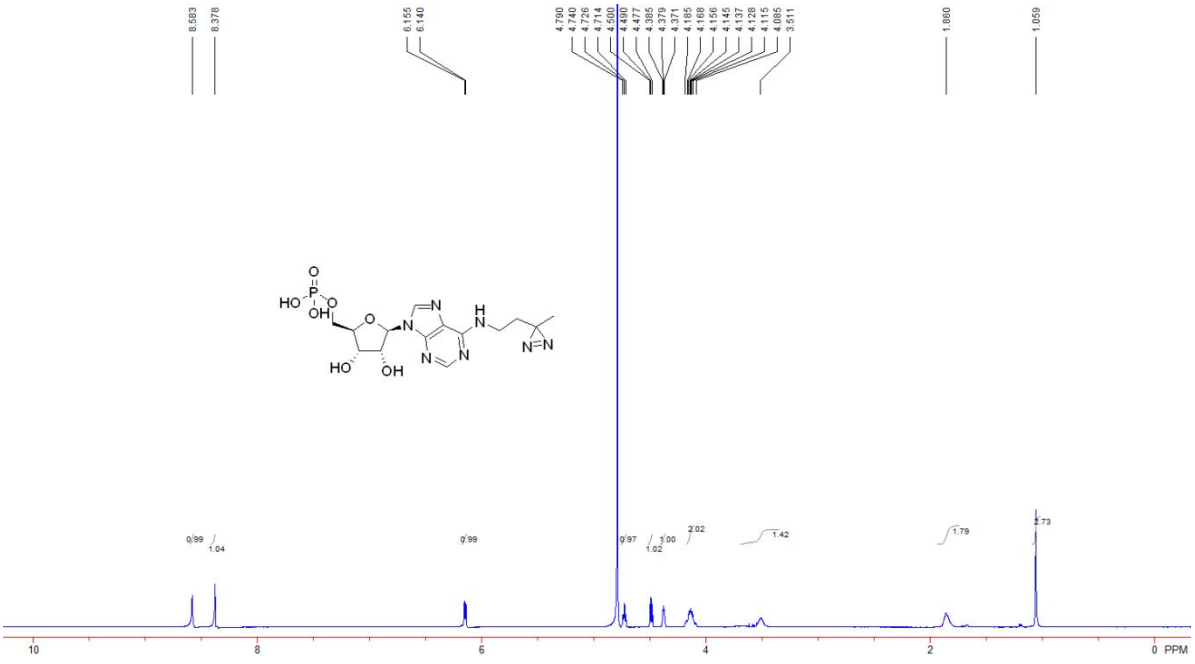

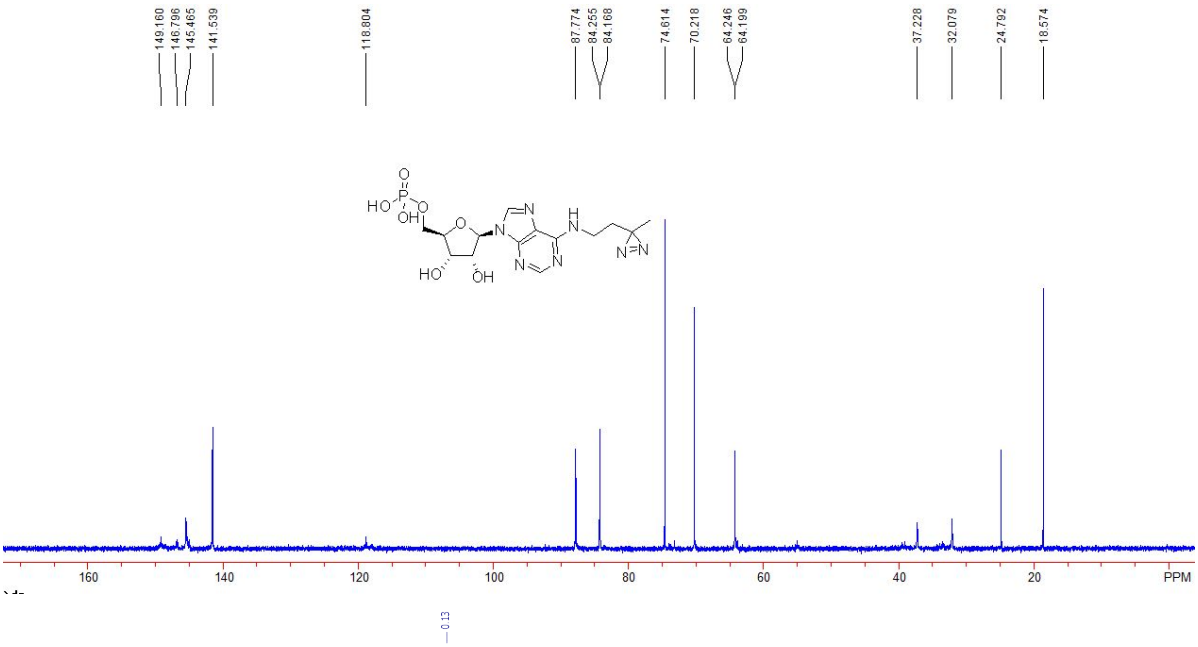

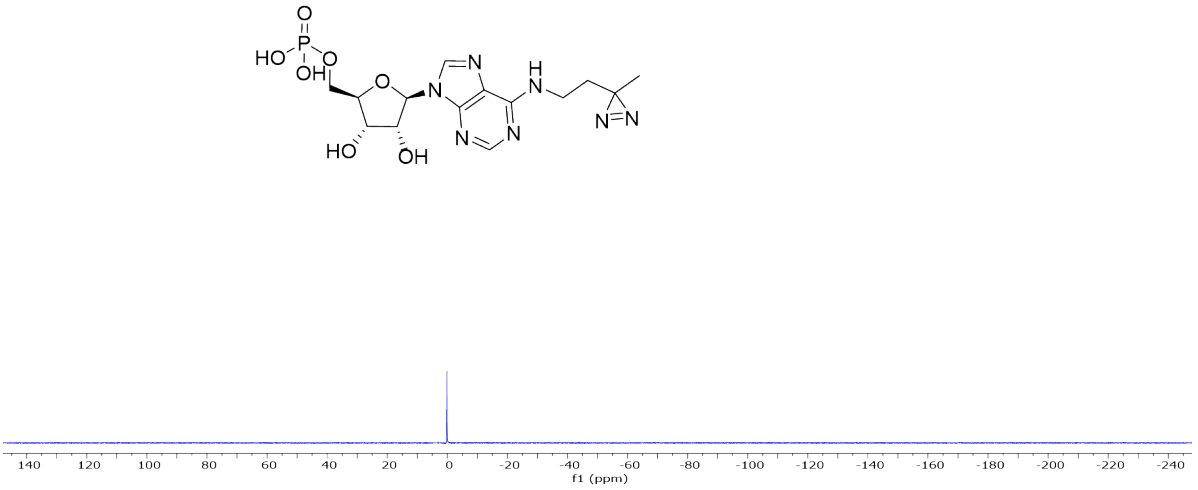

2-3

((2*R*,3*S*,4*R*,5*R*)-3,4-dihydroxy-5-(6-(((3-methyl-3*H*-diazirin-3-yl)methyl)amino)-9*H*-purin-9-yl)tetrahydrofuran-2-yl)methyl dihydrogen phosphate (2-3). A colorless solid, 44 mg, 70% yield; ^{1}H NMR (400 MHz, D_2O): δ 1.14 (s, 3H, CH_3), 3.73 (br, 2H, CH_2), 4.09-4.19 (m, 2H, CH_2), 4.38 (br, 1H, CH), 4.49 (t, 1H, J = 4.4 Hz, CH), 4.72 (t, 1H, J = 5.2 Hz, CH), 6.16 (d, 1H,

J = 4.8 Hz, CH), 8.41 (s, 1H, ArH), 8.59 (s, 1H, ArH); ^{13}C NMR (100 MHz, D_2O): δ 16.6, 25.4, 43.9, 64.2 (d, *J* = 4.6 Hz), 70.2, 74.6, 84.2 (d, *J* = 9.4 Hz), 87.9, 118.4, 141.5, 146.2, 146.9, 150.0; ; ^{31}P NMR (162 MHz, D_2O): δ 0.16; MS (ESI) *m/z*: 416.2 $(M+H)^+$.

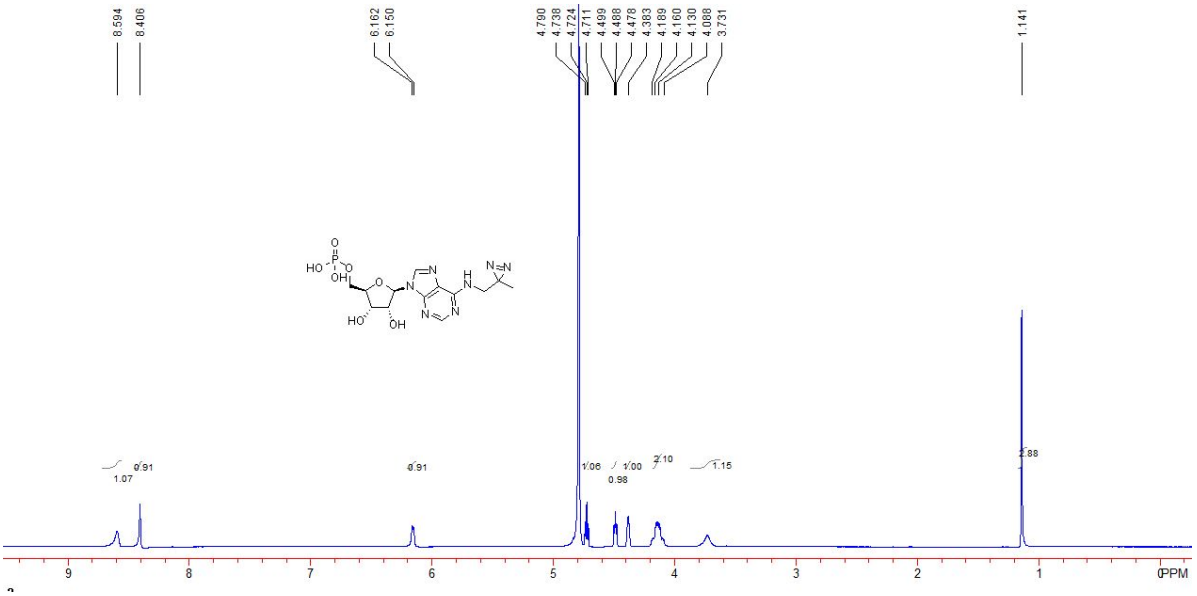

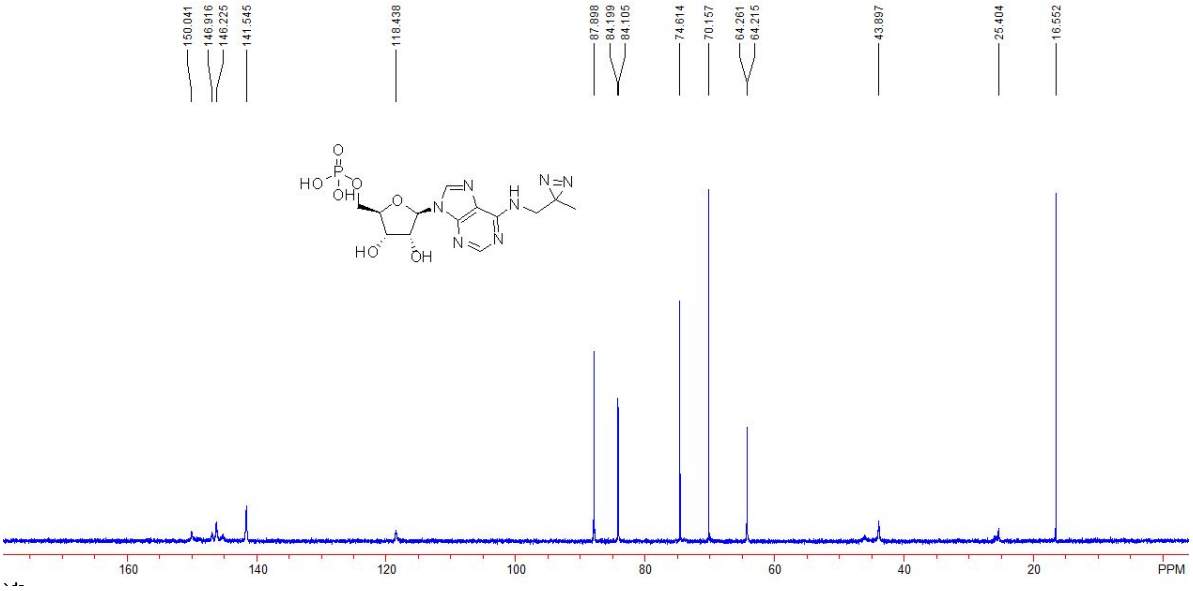

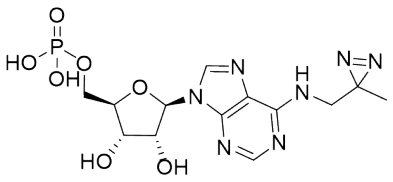

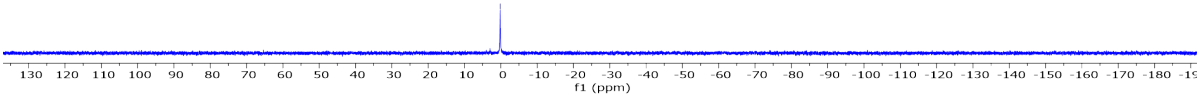

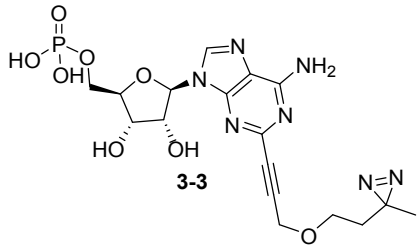

3-3

((2*R*,3*S*,4*R*,5*R*)-5-(6-amino-2-(3-(2-(3-methyl-3*H*-diazirin-3-yl)ethoxy)prop-1-yn-1-yl)-9*H*-purin-9-yl)-3,4-dihydroxytetrahydrofuran-2-yl)methyl dihydrogen phosphate (3-3). A colorless solid, 51 mg, 70% yield; ^{1}H NMR (400 MHz, D_2O): δ 1.05 (s, 3H, CH_3), 1.73 (t, 2H, *J* = 5.6 Hz, CH_2), 3.58 (t, 2H, *J* = 5.6 Hz, CH_2), 4.08-4.20 (m, 2H, CH_2), 4.35-4.38 (m, 1H, CH), 4.46-4.49 (m, 3H, CH+CH_2), 4.68 (t, 1H, *J* = 5.2 Hz, CH), 6.09 (d, 1H, *J* = 5.2 Hz, CH), 8.61 (s, 1H, ArH); ^{13}C NMR (100 MHz, D_2O): δ 18.7, 25.0, 33.1, 57.7, 64.1 (d, *J* = 5.5 Hz), 65.6, 70.1, 74.6, 79.9, 84.0 (d, *J* = 7.9 Hz), 87.7, 88.2, 117.5, 140.0, 141.8, 148.3, 151.9; ^{31}P NMR (162 MHz, D_2O): δ 0.17; MS (ESI) *m/z*: 484.1 $(M+H)^+$.

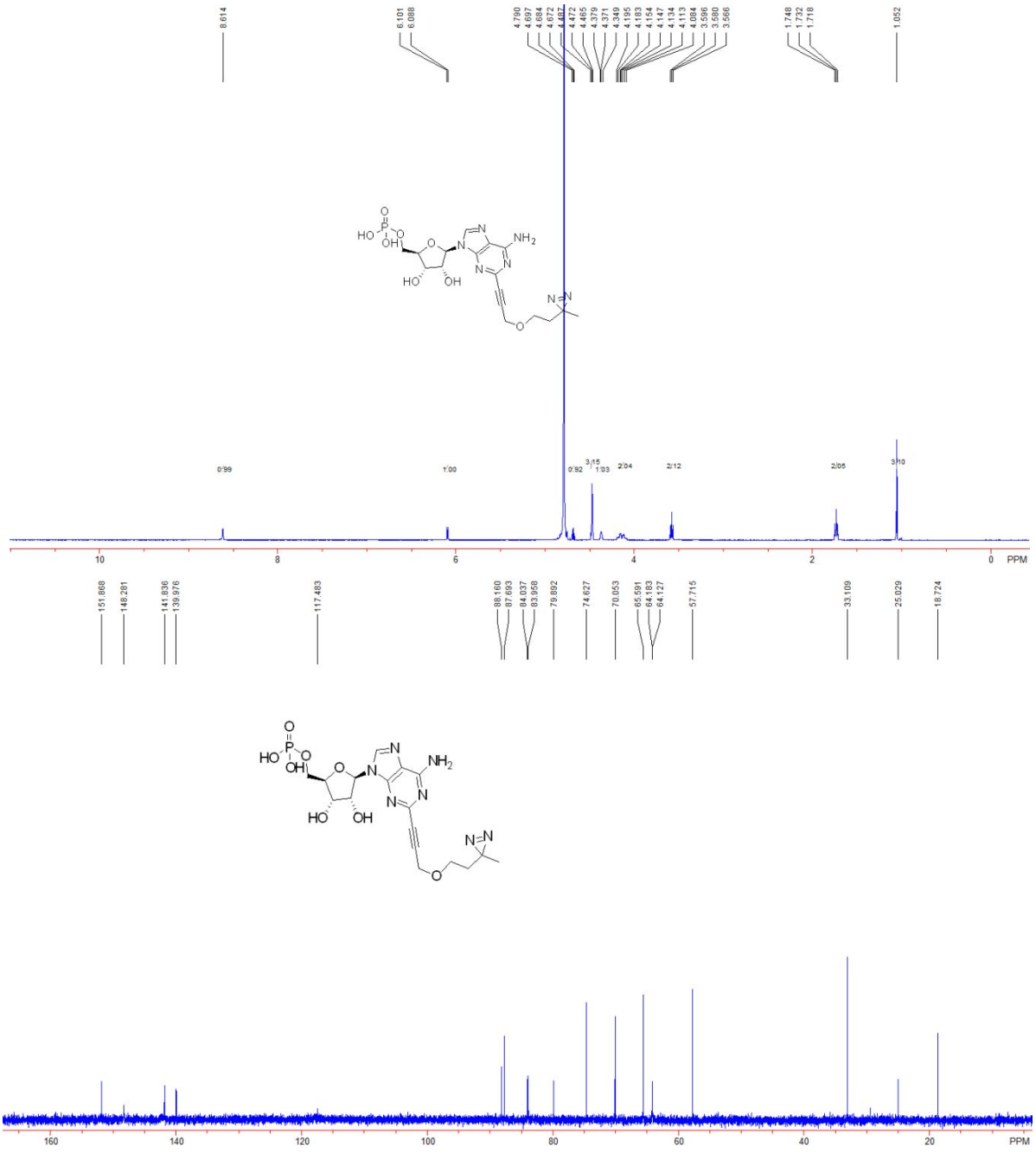
8.614
6.101
6.088
4.790
4.697
4.684
4.672
4.462
4.472
4.465
4.379
4.371
4.349
4.195
4.183
4.154
4.147
4.134
4.113
4.084
3.596
3.580
3.566
1.748
1.732
1.718
1.052
0.99
1.00
0.92
3.15
1.03
2.04
2.12
2.05
3.10
10
8
6
4
2
0
PPM
151.868
148.281
141.836
139.976
117.483
88.160
87.693
84.037
83.958
79.892
74.627
70.053
65.591
64.183
64.127
57.715
33.109
25.029
18.724
160
140
120
100
80
60
40
20
PPM

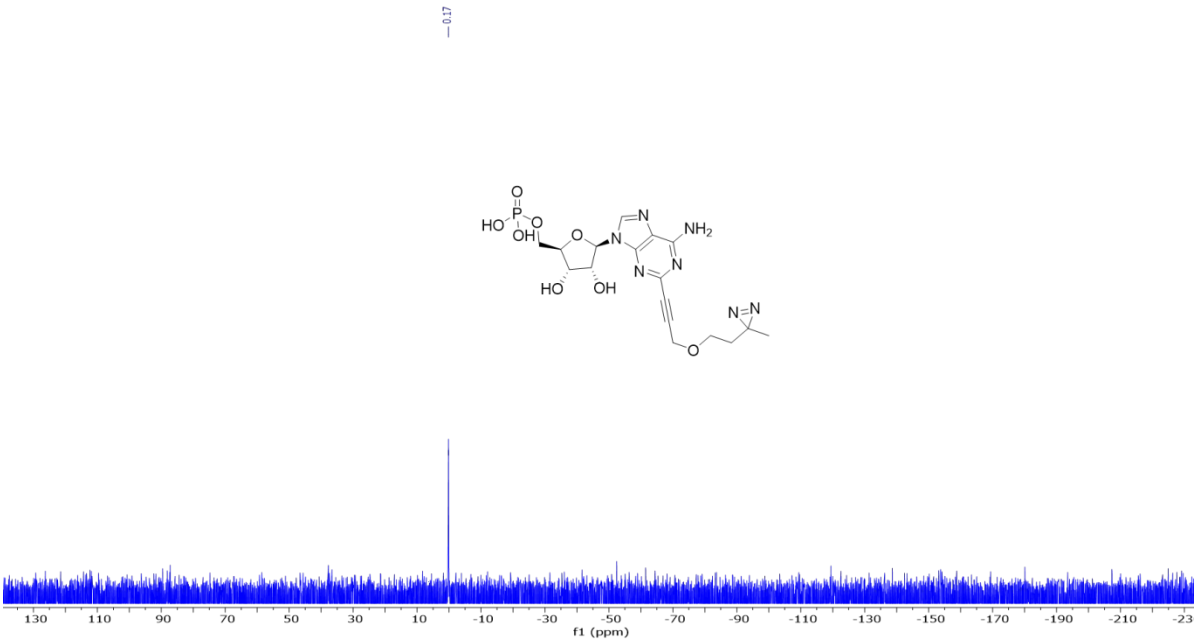

*General procedure for the synthesis of compound **1, 2 or 3***: To a stirred solution of **1-3, 2-3 or 3-3** (0.1 mmol, 1.0 eq) in dried DMF (2 mL) were added 1,1-carbonyldiimidazole (CDI) (63 mg, 0.50 mmol, 5 eq) and triethylamine (23 μL, 0.16 mmol. 1.6 eq). The reaction mixture was stirred at room temperature for 10 hours, and then quenched with 0.1 mL dried methanol. The solvent was removed under vacuum and the residue was co-evaporated 3 times each with 1 mL of dried DMF. The activated 5′-AMP analogue was dissolved in dried DMF (1 mL) and **3′-N_3-NMN** (54 mg, 0.15 mmol, 1.5 eq) was added. After stirring at room temperature for 4 days, H_2O was added to quench the reaction at 0°C. The resulting mixture was continued stirring at room temperature for 24 hours. The reaction was then concentrated *in vacuo* and the crude product was purified via preparative HPLC (C18 column, 150×10.0 mm, 5 μm) (mobile phase A: 0.1% formic acid (aq), mobile B: 0.1% formic acid in acetonitrile; flow rate = 2.0 mL min^{-1}; 0-2 min: 0-4% B, 2-4 min: 4-10% B, 4-6 min: 10-20% B, 6-12 min: 20-50% B, 12-17 min: 50-100% B, 17-20 min: 100-0% B) with detection of UV absorbance at 260 nm. Fractions containing the desired product were concentrated and lyophilized to yield the compound **1, 2 or 3**.

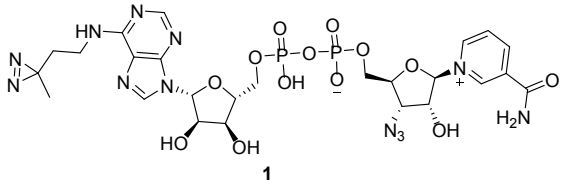

1

1-((2R,3R,4S,5S)-4-azido-5-(((((((2R,3S,4R,5R)-3,4-dihydroxy-5-(6-((2-(3-methyl-3H-diazirin-3-yl)ethyl)amino)-9H-purin-9-yl)tetrahydrofuran-2-yl)methoxy)(hydroxy)phosphoryl)oxy)oxidophosphoryl)oxy)methyl)-3-hydroxytetrahydrofuran-2-yl)-3-carbamoylpyridin-1-ium (1). A colorless solid, 32.2 mg, 42% yield; ^{1}H NMR (400 MHz, D_2O): δ 1.07 (s, 3H, CH_3), 1.79 (t, 2H, J = 6.8, CH_2), 3.45 (br, 2H, CH_2), 4.19-4.37 (m, 5H, $2CH_2$+CH), 4.37-4.51 (m, 3H, 3CH), 4.75 (t, 2H, J = 5.2 Hz, 2CH),

6.00-6.03 (m, 2H, 2CH), 8.14 (br, 1H, ArH), 8.18-8.21 (m, 1H. ArH), 8.56 (br, 1H, ArH), 8.83 (d, 1H, J = 7.6 Hz, ArH), 9.10 (d, 1H, J = 6.4 Hz, ArH), 9.29 (s, 1H, ArH); ^{13}C NMR (100 MHz, D_2O): δ 18.7, 25.4, 32.8, 35.8, 62.1, 65.0, 65.3, 70.2, 73.8, 77.7, 83.64-83.70 (m), 84.70-84.77 (m), 86.5, 99.4, 128.6, 133.6, 139.8, 142.2, 145.8, 152.6, 154.1, 164.9, 170.5; ^{31}P NMR (162 MHz, D_2O): δ -10.92 (br); HRMS (ESI) for $C_{25}H_{31}N_{12}Na_2O_{13}P_2^+$ $(M+2Na-H)^+$: Calcd.: 815.1404 Da; Obs: 815.1418 Da.

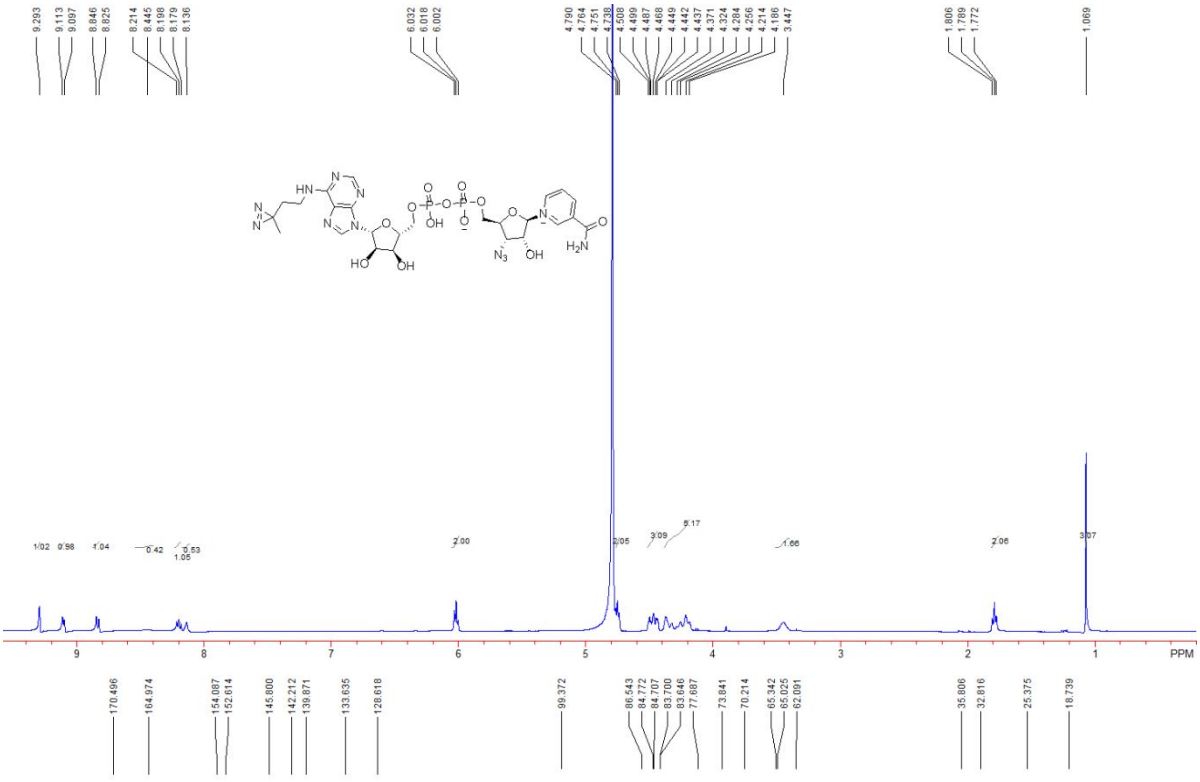

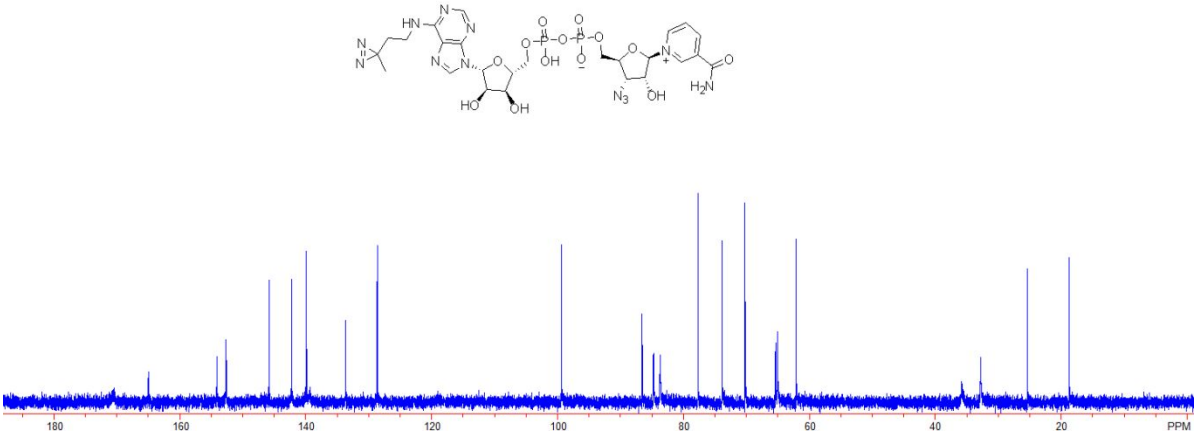

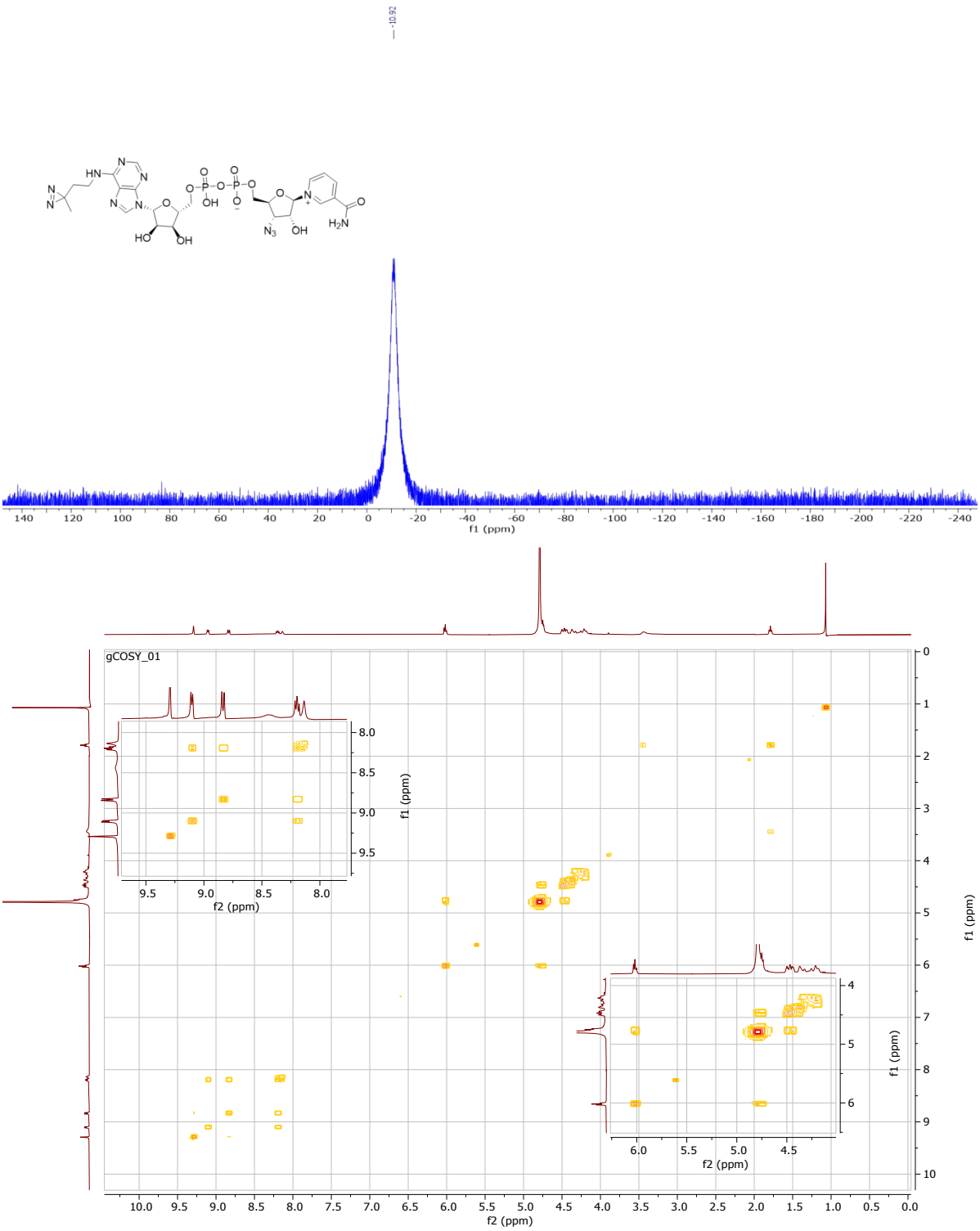
-10.92
f1 (ppm)
gCOSY_01
f2 (ppm)
f1 (ppm)

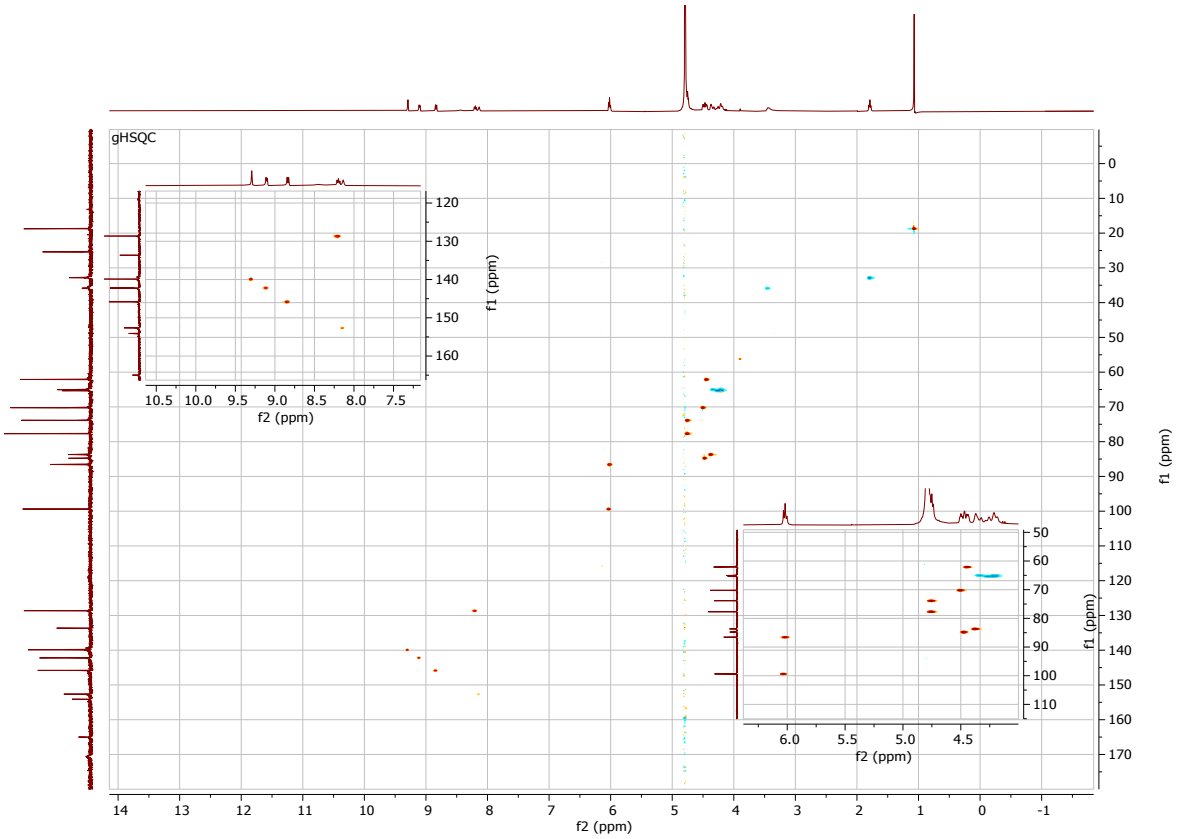

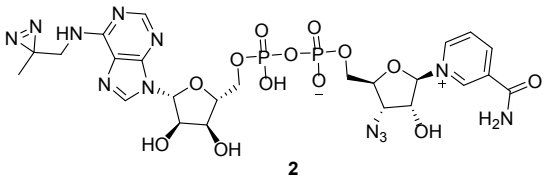

2

1-((2R,3R,4S,5S)-4-azido-5-(((((((((2R,3S,4R,5R)-3,4-dihydroxy-5-(6-(((3-methyl-3H-diazirin-3-yl)methyl)amino)-9H-purin-9-yl)tetrahydrofuran-2-yl)methoxy)(hydroxy)phosphoryl)oxy)oxidophosphoryl)oxy)methyl)-3-hydroxytetrahydrofuran-2-yl)-3-carbamoylpyridin-1-ium (2). A colorless solid, 28.7 mg, 38% yield; ^{1}H NMR (400 MHz, D_2O): δ 1.14 (s, 3H, CH_3), 3.68 (br, 2H, CH_2), 4.19-4.37 (m, 5H, $2CH_2$+CH), 4.44-4.46 (m, 2H, 2CH), 4.50 (t, 1H, J = 4.4 Hz, CH), 4.73-4.79 (m, 2H, 2CH, overlap with the solvent residue peak), 6.00-6.02 (m, 2H, 2CH), 8.16 (s, 1H, ArH), 8.19-8.23 (m, 1H, ArH), 8.41 (br, 1H, ArH), 8.86 (d, 1H, J = 8.0 Hz, ArH), 9.08 (d, 1H, J = 6.0 Hz, ArH), 9.29 (s, 1H, ArH); ^{13}C NMR (100 MHz, D_2O): δ 16.8, 26.5, 42.2, 62.2, 65.0-65.1(m), 65.3-65.4 (m), 70.2, 73.8, 77.7, 83.6-83.7 (m), 84.7-84.8 (m), 86.5, 99.4, 118.8, 128.6, 133.8, 139.5, 139.8, 142.3, 145.9, 152.5, 154.0, 165.1, 170.9; ^{31}P NMR (162 MHz, D_2O): δ -11.33 (br); HRMS (ESI) for $C_{24}H_{29}N_{12}Na_2O_{13}P_2^+$ $(M+2Na-H)^+$: Calcd.: 801.1248 Da; Obs: 801.1272 Da.

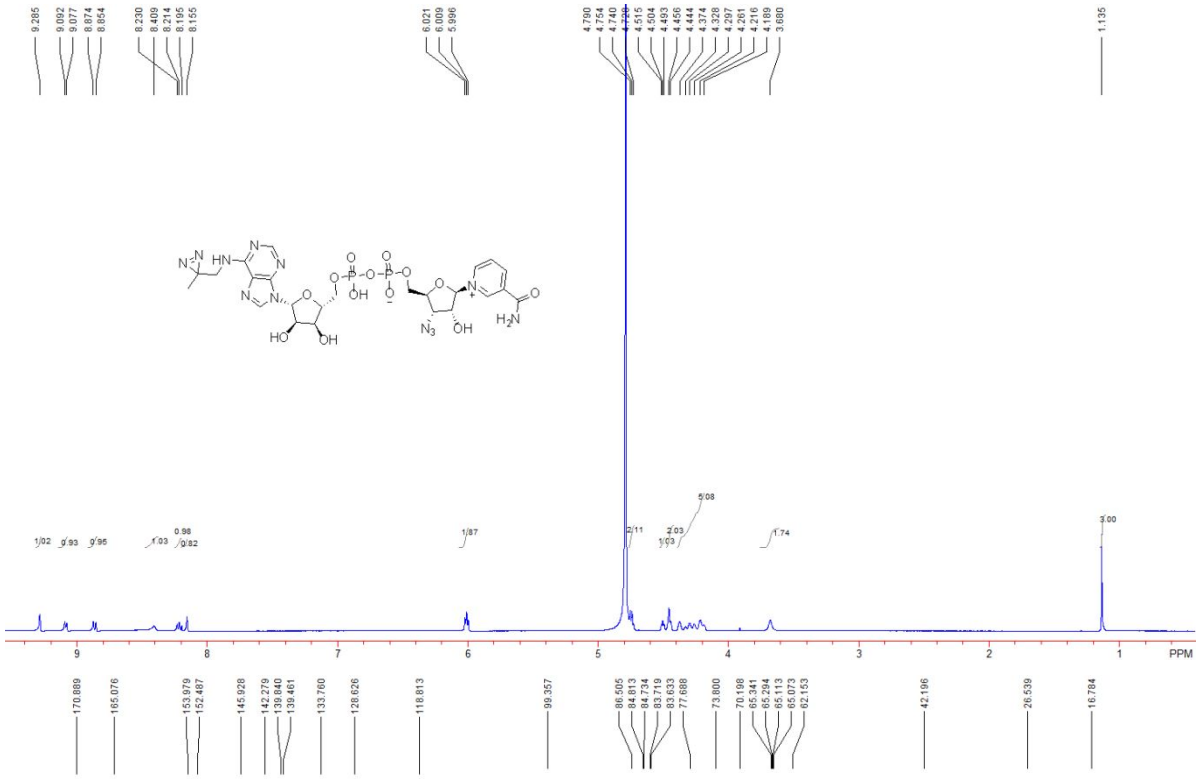
9.285
9.092
9.077
8.874
8.854
8.230
8.409
8.214
8.196
8.155
6.021
6.009
5.996
4.790
4.754
4.740
4.515
4.504
4.493
4.456
4.444
4.374
4.328
4.297
4.261
4.216
4.189
3.880
1.135
1.02
0.93
0.95
1.03
0.98
0.82
1.87
2.11
2.03
1.03
5.08
1.74
3.00
PPM

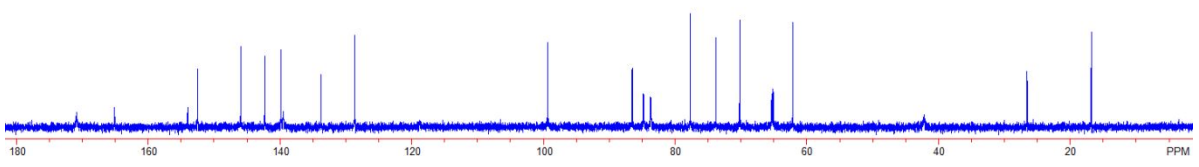
170.889
165.076
153.979
152.487
145.928
142.279
139.840
139.461
133.760
128.626
118.813
99.357
86.505
84.813
84.734
83.719
83.633
77.688
73.800
70.198
65.341
65.294
65.113
65.073
62.153
42.196
26.539
16.784

PPM

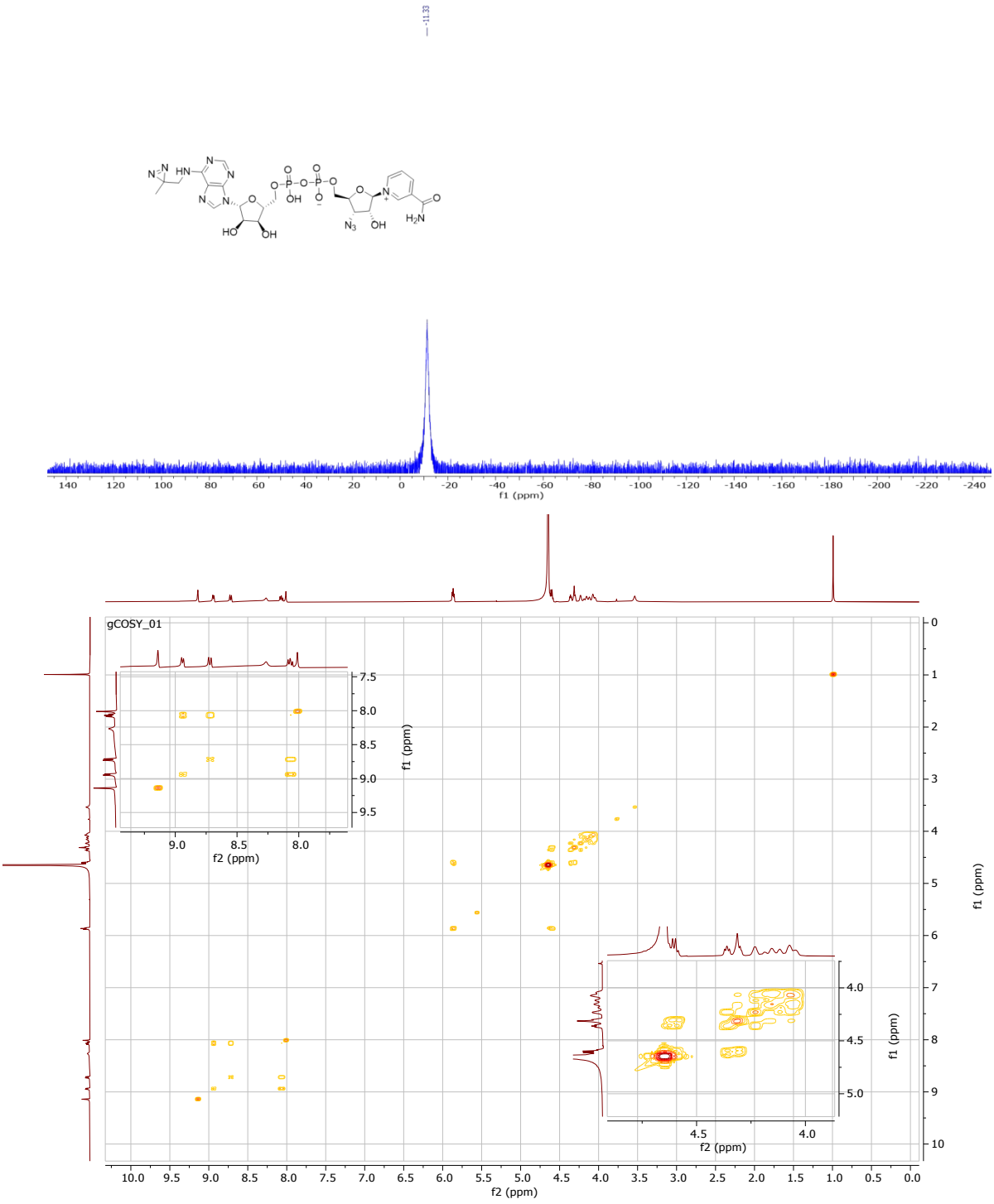
-11.33
f1 (ppm)
gCOSY_01
f2 (ppm)
f1 (ppm)

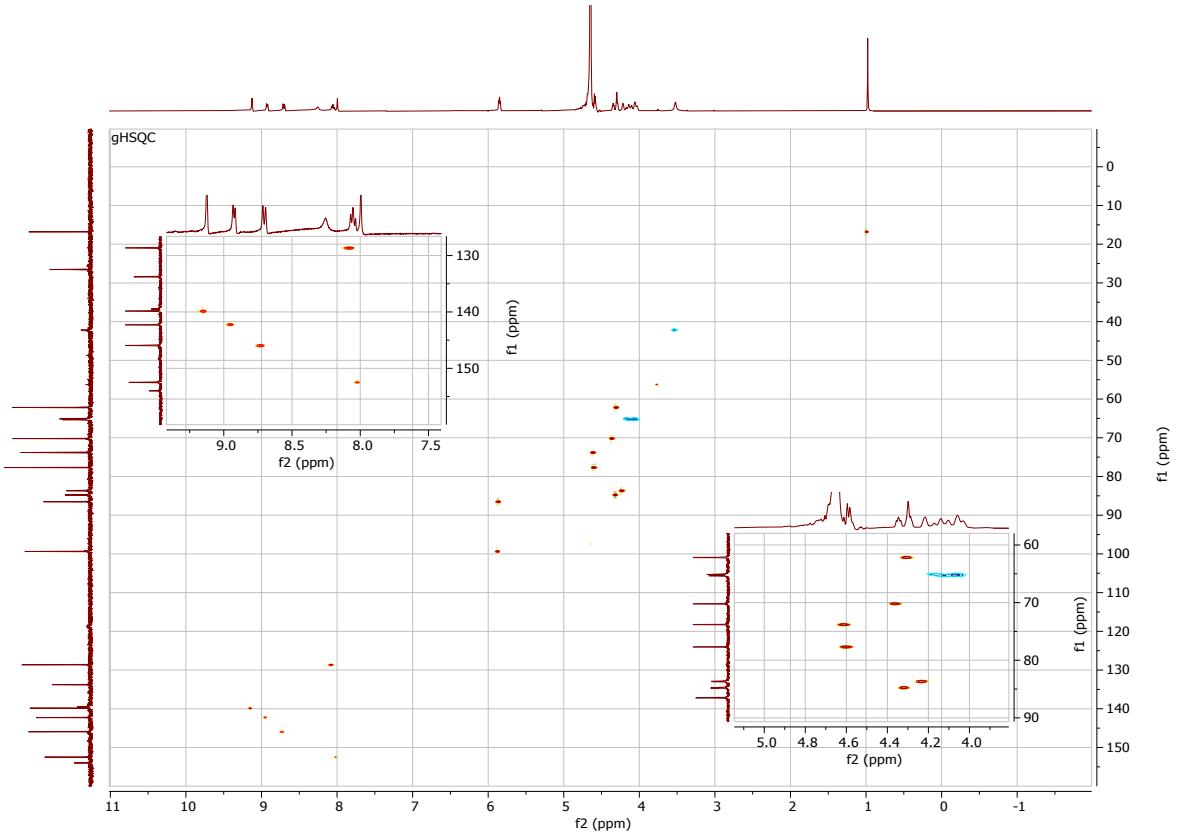

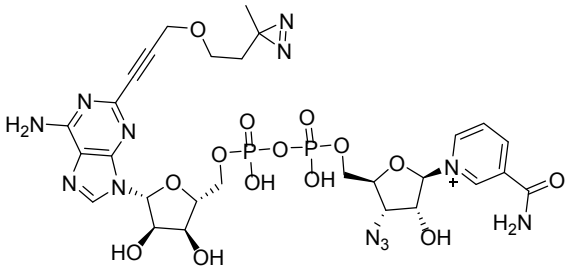

3

1-((2R,3R,4S,5S)-5-(((((((2R,3S,4R,5R)-5-(6-amino-2-(3-(2-(3-methyl-3H-diazirin-3-yl)ethoxy)prop-1-yn-1-yl)-9H-purin-9-yl)-3,4-dihydroxytetrahydrofuran-2-yl)methoxy)(hydroxy)phosphoryl)oxy)oxidophosphoryl)oxy)methyl)-4-azido-3-hydroxytetrahydrofuran-2-yl)-3-carbamoylpyridin-1-ium (3). A colorless solid, 28.9 mg, 35% yield; ^{1}H NMR (400 MHz, D_2O): δ 1.08 (s, 3H, CH_3), 1.76 (t, 2H, J = 6.0 Hz, CH_2), 3.59 (t, 2H, J = 6.0 Hz, CH_2), 4.18-4.33 (m, 4H, $2CH_2$), 4.40 (br, 1H, CH), 4.46-4.53 (m, 5H, 3CH+CH_2), 4.74-4.79 (m, 2H, 2CH, overlap with the solvent residue peak), 6.04-6.07 (m, 2H, 2CH), 8.24-8.29 (m, 1H, ArH), 8.65 (br, 1H, ArH), 8.94 (d, 1H, J = 8.0 Hz, ArH), 9.13 (d, 1H, J = 6.0 Hz, ArH), 9.35 (s, 1H, ArH); ^{13}C NMR (100 MHz, D_2O): δ 18.8, 25.1, 33.1, 57.8, 62.3, 65.0-65.2 (m), 65.5, 70.1, 74.1, 77.7, 81.3, 83.8-83.9 (m), 84.8-84.9 (m), 86.4, 87.2, 99.3, 128.7, 133.8, 139.9, 141.9, 142.3, 146.1, 153.1, 165.2; ^{31}P NMR (162 MHz, D_2O): δ -10.93 (br); HRMS (ESI) for $C_{28}H_{33}N_{12}Na_2O_{14}P_2^+$ $(M+2Na-H)^+$: Calcd.: 869.1510 Da; Obs: 869.1483 Da.

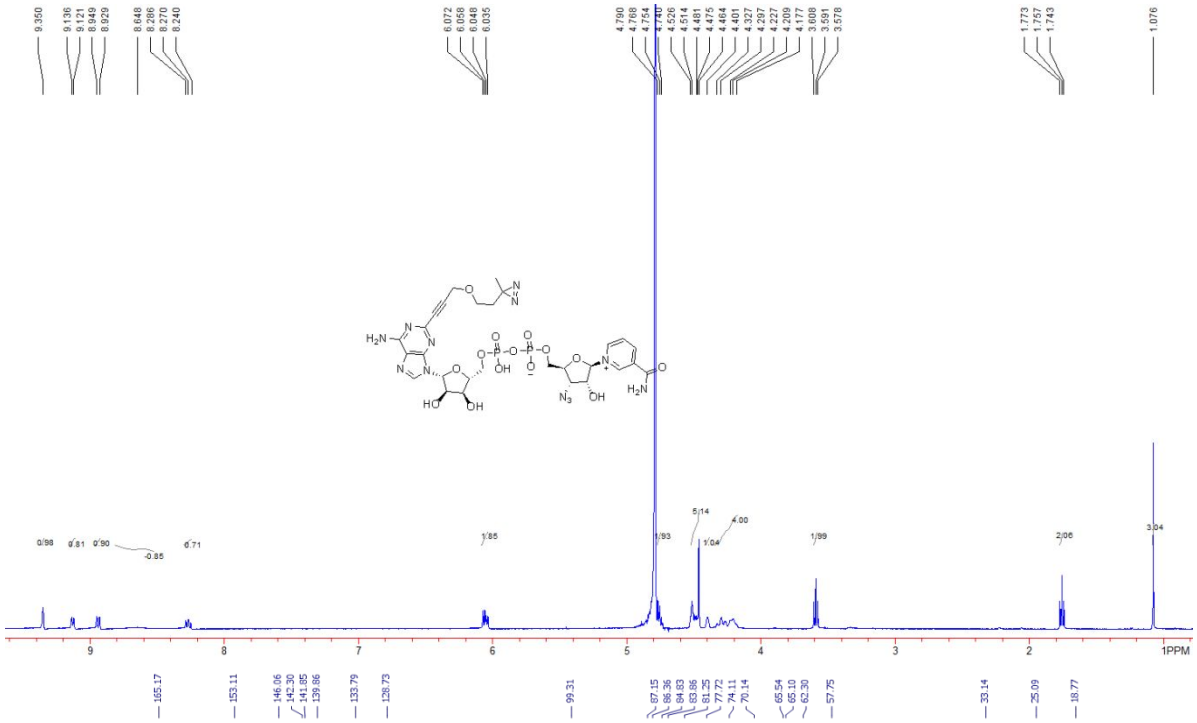
9.350
9.136
9.121
8.944
8.929
8.648
8.286
8.270
8.240
6.072
6.058
6.048
6.035
4.790
4.768
4.754
4.740
4.526
4.514
4.481
4.475
4.464
4.401
4.327
4.297
4.227
4.209
4.177
3.608
3.591
3.578
1.773
1.757
1.743
1.076
0.98
0.81
0.90
0.85
0.71
1.85
1.93
5.14
1.04
4.00
1.99
2.06
3.04
9
8
7
6
5
4
3
2
1PPM
165.17
153.11
146.06
142.30
141.65
139.86
133.79
128.73
99.31
87.15
86.36
86.03
83.86
81.25
77.72
74.11
70.14
65.54
65.10
62.30
57.75
33.14
25.09
18.77

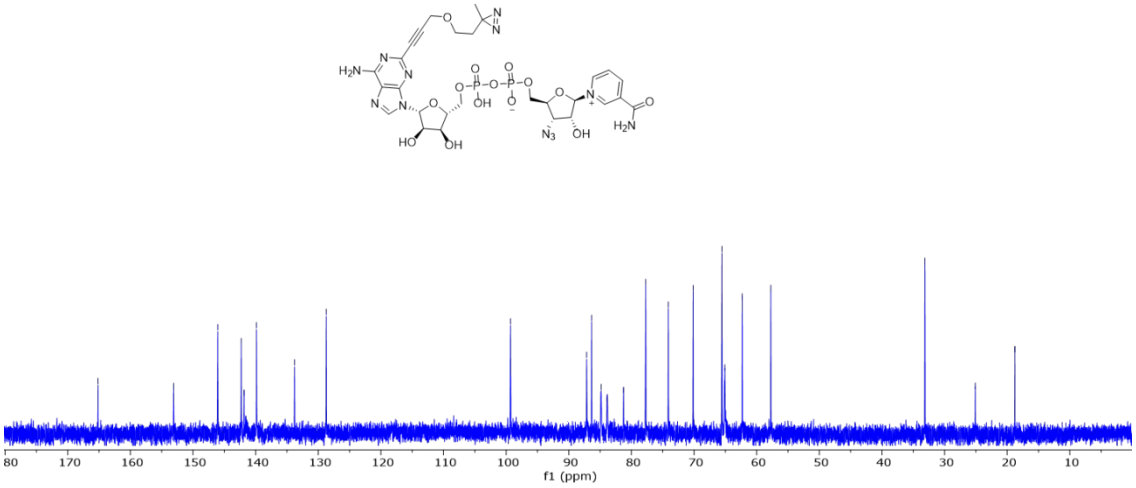
80
170
160
150
140
130
120
110
100
90
80
70
60
50
40
30
20
10
f1 (ppm)

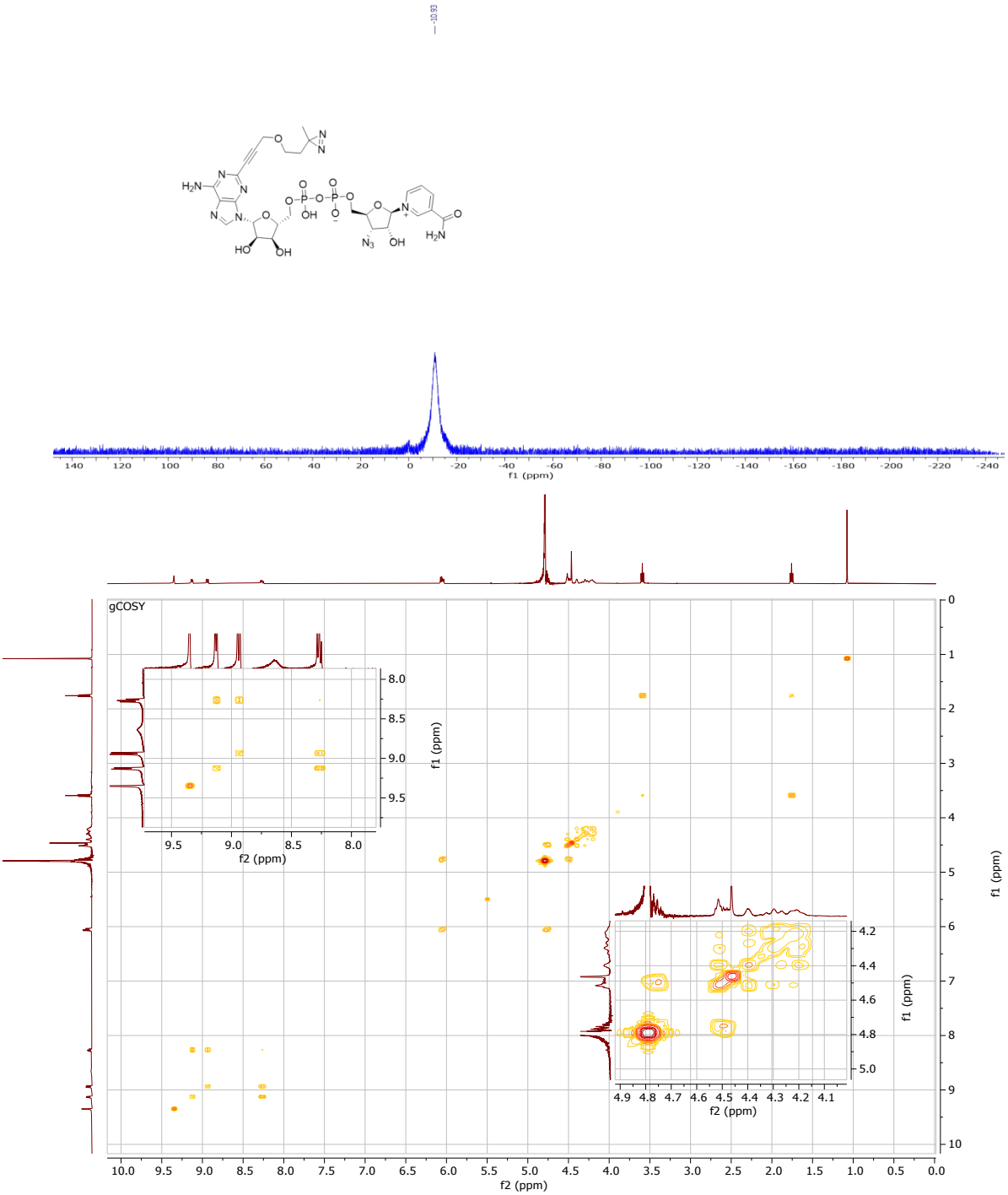
gCOSY
f1 (ppm)
f2 (ppm)

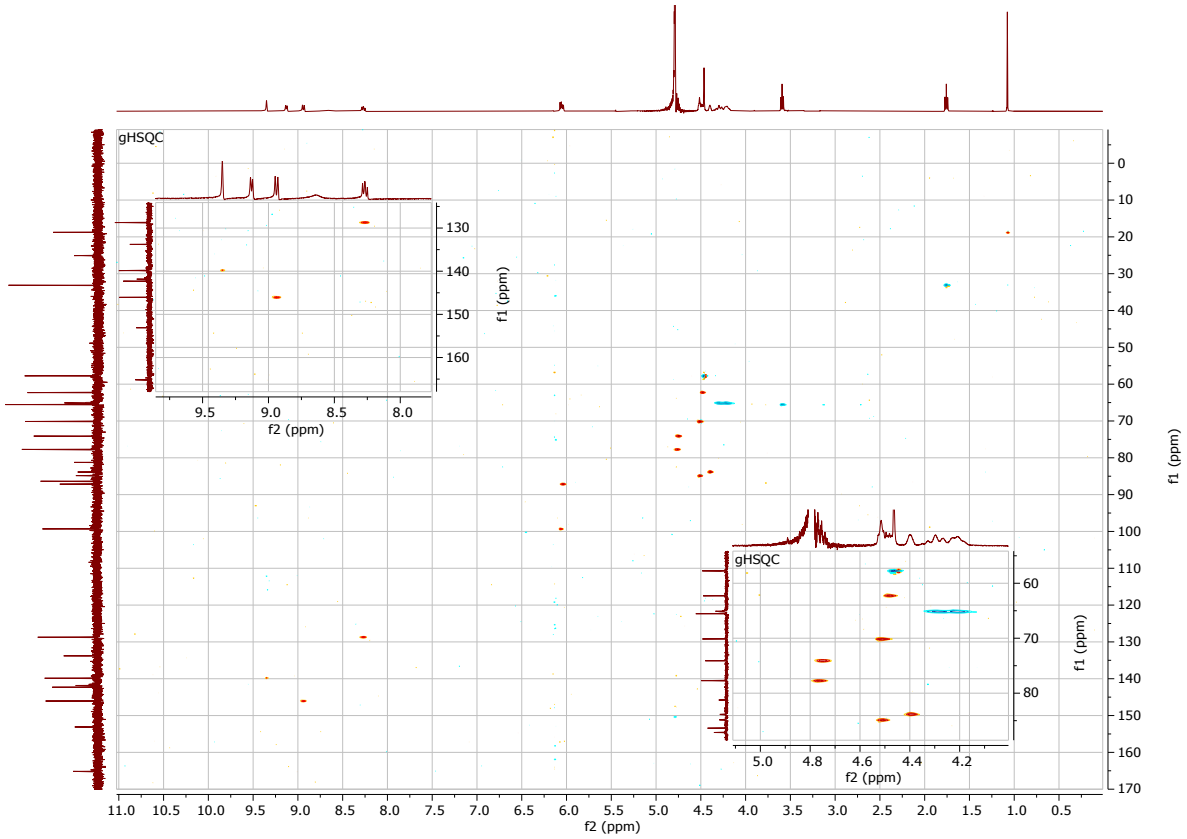

References

[1] Zhang, X.-N., Cheng, Q., Chen, J., Lam, A. T., Lu, Y., Dai, Z., Pei, H., Evdokimov, N. M., Louie, S. G., and Zhang, Y. (2019) A ribose-functionalized NAD+ with unexpected high activity and selectivity for protein poly-ADP-ribosylation, *Nature communications 10*, 4196.

[2] Tucker, J. A., Bennett, N., Brassington, C., Durant, S. T., Hassall, G., Holdgate, G., McAlister, M., Nissink, J. W., Truman, C., and Watson, M. (2012) Structures of the human poly (ADP-ribose) glycohydrolase catalytic domain confirm catalytic mechanism and explain inhibition by ADP-HPD derivatives, *PloS one 7*, e50889.

[3] Patel, C. N., Koh, D. W., Jacobson, M. K., and Oliveira, M. A. (2005) Identification of three critical acidic residues of poly(ADP-ribose) glycohydrolase involved in catalysis: determining the PARG catalytic domain, *Biochem. J. 388*, 493-500.

[4] Kim, I. K., Kiefer, J. R., Ho, C. M., Stegeman, R. A., Classen, S., Tainer, J. A., and Ellenberger, T. (2012) Structure of mammalian poly(ADP-ribose) glycohydrolase reveals a flexible tyrosine clasp as a substrate-binding element, *Nat Struct Mol Biol 19*, 653-656.

[5] Rueden, C. T., Schindelin, J., Hiner, M. C., DeZonia, B. E., Walter, A. E., Arena, E. T., and Eliceiri, K. W. (2017) ImageJ2: ImageJ for the next generation of scientific image data, *BMC Bioinformatics 18*, 529.